**Title**
Neural Stem Cell-Derived Factors Mediate Neurovascular Regeneration in Ischemic Stroke



**Author**
Zhao, Handi

**Publication Date**
2019

Peer reviewed|Thesis/dissertation

UNIVERSITY OF CALIFORNIA

Los Angeles

# Neural Stem Cell-Derived Factors Mediate Neurovascular Regeneration in Ischemic Stroke

A thesis submitted in partial satisfaction

of the requirements for the degree

Master of Science in Physiological Science

by

Handi Zhao

2019

ABSTRACT OF THE THESIS

Neural Stem Cell-Derived Factors
Mediate Neurovascular Regeneration
in Ischemic Stroke

by

Handi Zhao

Master of Science in Physiological Science
University of California, Los Angeles, 2019
Professor Rachelle Hope Watson, Co-Chair
Professor Stanley Thomas Carmichael, Co-Chair

Stroke is a leading cause of adult disability without treatment for long-term recovery. Stroke itself induces a wide-range of repair mechanisms, including the proliferation and long-distance migration of immature neurons (neuroblasts) from the subventricular zone (SVZ) to peri-infarct tissue. These neuroblasts localize to angiogenic blood vessels, forming a neurovascular niche in the peri-infarct zone. The reciprocal signaling between neuroblasts and endothelial cells has not been clearly characterized. A genome-wide expression profiling of stroke-induced neuroblasts and angiogenic vessels in the neurovascular niche led to the discovery of three differentially-regulated ligands derived from neuroblasts. These ligands are Wingless 7a (Wnt7a),

pleiotrophin (PTN), and chemokine (C-C motif) ligand 9 (CCL9). Mechanistic gain- and loss-of function studies show Wnt7a, PTN, and CCL9 mediate neural and vascular repair in the subacute and chronic periods after an ischemic cortical stroke.

The thesis of Handi Zhao is approved.

Amy Catherine Rowat

Rachelle Hope Watson, Committee Co-Chair

Stanley Thomas Carmichael, Committee Co-Chair

University of California, Los Angeles

2019

## Table of Contents

## List of Figures

## List of Tables

Acknowledgements

I wish to acknowledge my mentor, Dr. S. Thomas Carmichael, and all members of the Carmichael lab for their support, guidance, and assistance. I would also like to thank the members of my thesis committee for their time and effort during the thesis approval process. I would like to acknowledge Andrew Brumm and Tamal B. Lengning for their ideas, experiments, and results that supported the work of this study. Andrew Brumm conducted the microarray and bioinformatics studies and analysis (pages 9 and 25). As part of his doctoral studies, Tamal B. Lengning designed and performed the candidate gene studies and developed analysis methods that led to the quantifications reported on pages 10-16.

I would like to acknowledge the funding provided by the National Institute of Health and the Adelson Research Foundation for supporting this project.

## Introduction

Stroke is a leading cause of death and adult disability without treatment for long-term recovery. Stroke ranks number 5 as the leading cause of death in the United States and number 2 worldwide.[1] Among clinical stroke types, ischemic stroke accounts for 87% of all strokes and is caused by a clot in a cerebral blood vessel that leads to neural cell and tissue damage.[2] There is a very limited window for stroke treatment. Current treatment methods all aim to return blood flow to the damaged tissue. One common treatment relies on the use of tissue plasminogen activator (tPA), which converts the enzyme plasminogen to plasmin to break down the clot. The second common treatment is endovascular thrombectomy, which is the physical removal of the clot using a stent retriever. Both treatments are widely used in stroke clinics; however, these procedures must be applied within 24 hours of stroke onset (tPA within 3-4.5 hours; thrombectomy within 24 hours).[3] Despite efforts to restore neural functions, there are no treatment currently available for long-term recovery from stroke.

Ischemic stroke results from cessation of blood flow and is characterized by a distinct area of necrotic tissue termed the infarct core. Surrounding the infarct core is a hypoperfused region known as the ischemic penumbra, where the tissue is damaged and at risk of complete cell death.[4] Blood flow to the penumbra continues to deliver oxygen and glucose to the surviving cells. However, this region is subject to a wave of deleterious inflammatory response and metabolic stress propagated from the core, leading to the expansion of ischemic injury and the subsequent worsening of clinical outcome within 24 hours to 7 days after stroke onset.[4,5] This ischemic recruitment process establishes a time frame for reperfusion therapies to save the penumbral tissue, making this area a target for extending the therapeutic window, brain plasticity, and neuroprotective and neurorepair treatments.[4,5] Deficits after stroke improve with time, suggesting

that the brain has at least some capacity for repair.[6] In stroke patients, microvessel density in the penumbra tends to increase and this increase is correlated with longer survival. This neovascularization represents one mechanism that might mediate the repair process.[7,8]

In the adult brain, post-stroke neural repair involves a number of processes of anatomical and functional changes, including axonal sprouting, remapping of cortical networks, angiogenesis, and neurogenesis.[8] Angiogenesis is defined as the growth and remodeling of the vasculature. Neurogenesis is the proliferation and differentiation of neural stem cells into neuronal and glial lineages.[9] Post-stroke angiogenesis and neurogenesis have been demonstrated in rodents, primates and humans.[6,10] In adult rodents and mammalians, neurogenesis occurs in the subventricular zone (SVZ) in the lateral region of the ventricles and the subgranular zone (SGZ) of the hippocampus. Stem cells in the SGZ differentiate and migrate to the dentate gyrus granule cell layer and is important for learning and memory.[11,12] Neurogenesis in the SVZ gives rise to neuroblasts, which are immature neurons that migrate in chains along blood vessels to the olfactory bulb in a process known as the rostral migratory stream. Once neuroblasts reach the olfactory bulb, they detach and differentiate into periglomular and granule neurons, but only some survive long-term and integrate into the circuitry.[13,14] The association between the neuroblasts and the blood vessels guiding them to the olfactory bulb are mediated by molecules that induce cell-to-cell interaction.[15] These processes that normally occur in the adult brain indicate the brain has some capacity for repair and plasticity.

In rodent models of stroke, focal ischemia potently stimulates SVZ cell proliferation and neurogenesis that gives rise to new neurons in the regions adjacent to the infarct cortex.[11,16–20] A closer examination of these stroke-responsive neuroblasts reveals a close association with angiogenic vessels. Large clusters of neuroblasts localizes to newly born endothelial cells in the

peri-infarct, forming a regenerative neurovascular niche.[19,21–23] These angiogenic vessels act as a scaffold that provide directional guidance for the neuroblasts to the peri-infarct region. Systemic administration of pro- and anti-angiogenic factors induce or inhibit the growth of new vessels, respectively, and neuroblast migration to the peri-infarct core is modulated accordingly. These stroke-responsive neuroblasts arise from the SVZ and is diverted away from their typical path to the olfactory bulb. This stimulation of long-distance migration of SVZ-derived neural progenitor cells to the stroke peri-infarct cortex suggests that post-stroke angiogenesis and neurogenesis are casually linked. Furthermore, in human stroke, there is evidence of stroke-induced neurogenesis with new born neurons residing in close proximity to the blood vessels in the ischemic penumbra.[10] These implications suggest stimulating post-stroke neurogenesis and angiogenesis to promote the proliferation and migration of neural progenitor cells may contribute to functional recovery. However, molecular mediators of the interaction between migrating neuroblasts and the remodeling vasculature in the peri-infarct niche are not known.

A former graduate student in the Carmichael Laboratory previously established a microarray and bioinformatics dataset that described molecular pathways potentially involved in the bidirectional signaling between stroke-responsive neuroblasts and angiogenic blood vessels. The analysis consisted of gene expression profiles of migrating immature neurons derived from the SVZ and endothelial cells in the peri-infarct cortex. These gene systems code for secreted or membrane-bound products that can signal to endothelial cells to promote angiogenesis and migration of the neuroblasts. Three candidate gene sets were selected based on the amount and statistical significance of gene expression change and available literature that support a functional role in vascular or stem cell progenitor differentiation. This study aims to determine the functional

role of CCL9, Wnt7a, and PTN in post-stroke angiogenesis and neurogenesis, and whether their modulation of these processes contribute to functional recovery after stroke.

CCL9 is a chemokine ligand produced in macrophages, osteoclasts, and functions as a cell survival factor. Chemokines are known to induce directed chemotaxis of responsive cells and can promote cell migration during brain development.[24] Some chemokines are released as an inflammatory response to injury; however, several other chemokines, such as stromal cell-derived factor 1 (SDF-1$\alpha$) are known to promote neuronal cell migration during normal and post-stroke angiogenesis in the peri-infarct zone.[21,25] CCL9 is largely linked to tumor angiogenesis and cell growth.[26] In vitro, the human homolog of CCL9, CCL15, increase endothelial cell proliferation and differentiation through the chemokine (C-C motif) receptor 1 (CCR1).[27] Current literature has linked CCL9 to tumor angiogenesis and expansion, however, its role in CNS and neural repair is not clearly understood, making this a novel target for potential regenerative therapies.

PTN is a heparin-binding cytokine normally expressed in mature neurons and has mitogenic activity that promotes brain capillary endothelial cell proliferation.[28,29] Similar to CCL9, PTN is overexpressed in tumors and stimulates tumor angiogenesis and endothelial cell proliferation after myocardial infarctions.[30,31] Additionally, PTN induces neurite outgrowth and vasculogenesis during development and has post-developmental neurotrophic and neuroprotective functions.[28,32] After acute ischemic brain injury, the PTN gene is upregulated in microvasculature, macrophages, and astrocytes in the peri-infarct cortex.[33] These evidences suggest PTN may be a key contributor to recovery of brain function after stroke.

Wnt7a has been extensively studied in angiogenesis and neurogenesis in the developing and adult central nervous system (CNS). Wnt7a stimulates neural progenitor proliferation and differentiation in the embryonic and neonatal mouse brain and can regulate multiple steps of

neurogenesis through canonical signaling via activation of β-catenin. Loss of Wnt7a lead to reduced neural stem cell self-renewal and decreased neuronal maturation and differentiation, as well as defects in vascular formation and blood-brain barrier integrity.[34,35] These pro-angiogenic and neurogenic properties of Wnt7a, CCL9, and PTN suggest these targets are potentially important in regulating neural repair processes in the neurovascular niche after stroke.

## Materials and Methods

### *Animal Treatment and Microsurgeries*

### *Microarray and Bioinformatics Analysis*

Focal cortical strokes were produced in 2-month-old male doublecortin promoter-red fluorescent protein (DCX-RFP) transgenic mice (gift of Dr. E. Masliah, UCSD) using a model of permanent distal middle cerebral artery and transient (15 minutes) bilateral common carotid artery occlusion. Brains were collected 7 days after stroke and thin sections were stained for platelet endothelial cell adhesion molecule (PECAM) to label both remodeling (angiogenic) and mature blood vessels. Angiogenic vessels were identified based on their location within peri-infarct cortex (< 500um from the infarct core) and their larger, more disorganized morphology. PECAM+ endothelial cells from peri-infarct angiogenic blood vessels were isolated using a laser capture microdissection system (Molecular Devices). DCX-RFP+ neuroblasts adjacent to the angiogenic vessels were isolated using fluorescence-activated cell sorting. Isolated and amplified RNA were used to probe whole genome arrays (mouseRef-8, Illumina for neuroblasts, Agilent mouse arrays for vessels). Samples of 20 animals were used for gene expression study. Differential gene expression was assessed via contrast analysis using the LIMMA package. After linear model fitting, a Bayesian estimate of differential expression was calculated using a false discovery rate of 0.001%. Similar isolation and array analysis were performed with respective control cells: normal endothelial cells from cortex contralateral to the stroke, and normal neuroblasts that had migrated to the olfactory bulb. Bioinformatics analysis was completed at the Informatics Center for Neurogenetics and Neurogenomics (ICNN) at UCLA to determine which genes interact.

***Gain- and loss-of-function studies***

Lentiviruses with a EF1α promoter driving the expression of a BFP or GFP reporter and Wnt7a, PTN, or CCL9 was injected into the left motor cortex of 2-month-old male C56BL/6J mice (Jackson Lab) 14 days before stroke [anterior/posterior (A/P): 0 mm, medial/lateral (M/L): -0.5mm, -2.5mm, dorsal/ventral (D/V): 0.75mm]. Rose Bengal dye [10mg/ml] was injected at a volume of 10μL/g intraperitoneally and allowed to diffuse and enter the blood stream for 5 minutes. A fixed light source (180mV) is placed in the left motor cortex (M/L: -1.5mm; 18 minutes). 2'-deoxy-5'-ethynyluridine (EdU; Carbosynth NE08701) is given in drinking water at 200μg/ml starting 24 hours before stroke for 7 consecutive days after stroke. Body temperature was maintained at 37.0 °C with a heating pad throughout the procedure.

***Tissue Processing and Immunohistochemistry***

Brains were perfused with 2% paraformaldehyde using the periodate-lysine-paraformaldehyde (PLP) perfusion followed by 24 hours of post-fixation as described.[36] Tissues were cryosectioned into 40μm sections. Immunohistochemistry: Day 1: tissues were rinsed in 0.02M potassium phosphate buffered saline (KPBS) and blocked for 45 minutes in 5% normal donkey serum (NDS) and 0.03% triton in 0.02M KPBS followed by overnight incubation in primary antibodies, 2% NDS, and 0.1% triton in 0.02M KPBS. Day 2: Tissues were incubated in a secondary antibody solution for 1 hour (Jackson ImmunoResearch) followed by a 10-minute wash in DAPI. EdU labeling: tissues were incubated for 30 minutes in EdU cocktail that consisted of 4mM copper sulfate, 100mM sodium ascorbate, 100mM tris-buffered saline pH 7.6, and 2μM sulfo-Cy5 azide (Lumiprobe, C3330). Primary antibodies: rat anti-CCL9 (Biorbyt A2444), rabbit anti-NeuN (Abcam, ab177487), guinea pig anti-DCX (Millipore EMD AB2253),

rabbit anti-Olig2 (Millipore EMD AB9610), rat-CD31 (BD Pharmingen, 553370), goat-PTN (Santa Cruz, sc-1394), mouse anti-Wnt7a (Santa Cruz, sc-365459), rat anti-GFAP (Life Technologies, 130300), goat anti-Iba1 (Abcam, ab5076)

***Behavior Assessment***

Mice ($n$ = 12) were tested on grid-walking and cylinder tests. Baseline motor function was measured 1 day before virus injection followed by a photothrombotic stroke as described previously. Both tests were measured at 1, 4, and 8 weeks post-stroke. For the grid-walk test, animals were placed on a metal grid and were allowed to move freely for 5 minutes of recording time. For the cylinder test, animals were placed inside a clear plastic cylinder and were allowed to explore during the 5-minute recording time.

***Data Analysis and Statistics***

Imaris Image Analysis Software was used to quantify neuron, neuroblast, endothelial cell, vessel, and microglia densities. Cortical DCX+/DAPI+/EdU+, NeuN+/EdU+ and CD31+/EdU+ cell and vessel densities were tested with one-way ANOVA. Behavior data was analyzed using two-way ANOVA. Microglia density and glut-1 expression were analyzed using Student's $t$-test.

## Results

### Microarray Dataset Presents Differentially Expressed Genes in Neuroblasts after Stroke

Doublecortin-promoter-red-fluorescence-protein (DCX-RFP) transgenic mice underwent a focal cortical stroke produced by a model of permanent distal middle cerebral artery and transient bilateral common carotid artery occlusion (MCAo) (Fig 1*A*). These mice were sacrificed at 7 days after stroke, a time of peak neurovascular association.[21] Expression profiles of angiogenic endothelial cells from the peri-infarct zone was compared with non-angiogenic endothelial cells from the contralateral hemisphere. Regenerating neuroblasts adjacent to the angiogenic vessels in the peri-infarct cortex was compared with the normally migrating neuroblasts in the olfactory bulb. A comparison of whole genome expression profiles show a set of genes with significant changes in expression (Fig 1*B*). A bioinformatic analysis then identified the protein products of gene sets that might interact. From this neurovascular interactome, we identified three differentially expressed ligands in regenerating neuroblasts that signal to their receptors on angiogenic vessels (Fig 1*B*). These ligand-receptor pairs include CCL9/CCR1, Wnt7a/Frizzled 5, and PTN/receptor protein tyrosine phosphatase (RPTPBβ/ζ). With the exception of CCL9, Wnt7a and PTN are both downregulated after stroke based on the microarray analysis (Table 1, CCL9: +3.040-fold change; Wnt7a: -0.591-fold change; PTN: -0.330-fold change). Expression of these genes in the brain were validated with immunohistochemistry. PTN is expressed in mature neurons in a naïve mouse (Fig 2*A*). Immunostaining validation shows decreased Wnt7a expression in stroke-responsive neuroblasts compared to its normal expression in neuroblasts in the olfactory bulb at 7 days after stroke as well as normal expression in mature neurons in a non-stroke control animal (Fig 2*C*). CCL9 expression was found to be upregulated in the peri-infarct region after stroke (Fig 2*B*). These

data confirm the expression of our genes of interest in the brain and specifically in neuronal cell types.

**Neuroblast-Derived Factors Regulate Neurogenesis after Cortical Ischemic Stroke**

A mechanistic overexpression and knockdown approach was used to examine the functional role of CCL9, Wnt7a, and PTN in the neurovascular niche after stroke. To induce overexpression of these genes, a lentivirus expressing the EF1a promoter drove the expression of CCL9, Wnt7a, or PTN (Fig 3*A*). The virus was injected into the motor cortex of 2-month-old C57BL/6 male mice 14 days before stroke (Fig 3*A*). Downregulation of these genes was completed using a microRNA (miR) construct also expressed under the EF1a promoter (Fig. 3*A*). Respective control groups for the overexpression and knockdown studies will be termed expression control and miR control. Expression of virus after 14 days is indicated by a blue fluorescent reporter (BFP) and is found in both mature neurons and astrocytes, as shown by co-labeled BFP+/NeuN+ and BFP+/GFAP+ cells, respectively (Fig. 3*B* and *C*). To mark proliferating cells, we provided a thymidine analogue, EdU, in drinking water for 8 consecutive days starting 1 day before stroke.

To elucidate the impact of these ligands on the ongoing cellular processes in the perilesional region after stroke, we used the photothrombosis (PT) stroke model to produce a localized ischemic cell death in the motor cortex. Similar to the MCAo model, this technique also leads to a hypoperfused region adjacent to the infarct core, mimicking the ischemic penumbra in human brain tissue after stroke (Fig 3*A*).[37] The PT model induces the migration of neural progenitor cells from the SVZ in a similar fashion as MCAo. To confirm this, we utilized Ascl1(Mash1)-CreERT2::tdTomato transgenic mice and administered tamoxifen for 5 consecutive days after stroke. Co-labeling of neural progenitor cell marker DCX and tdTomato at 3 and 10

days after stroke showed gradual migration of SVZ-derived neural progenitor cells from the SVZ to the peri-infarct region (Fig 4*A*, *B*).

Adult neurogenesis begins with neural stem cells that differentiate into neuroblasts at 1-2 weeks marked by the expression of DCX, followed by maturation into neurons which express nuclear antigen NeuN at 4-8 weeks.[38] To examine short term neurogenesis regulated by CCL9, Wnt7a, and PTN, we quantified the density of immature neuroblasts at 14 days after stroke. Regions used for quantification included the peri-infarct cortex, the white matter, as well as the SVZ to accurately evaluate the total number of migrating stroke-responsive neuroblasts (Fig. 5*A*). We used nuclear marker 4′,6-diamidino-2-phenylindole (DAPI) to localize single DCX+ cells. Co-labeling of DCX, DAPI, and EdU showed increased neuroblast density in CCL9 overexpressing animals, however, this effect was not statistically significant compared to expression control animals (expression CCL9: 35.11 ± 13.81 vs expression control: 12.76 ± 2.80 cells per $mm^2$; ANOVA: $P > 0.05$) (Fig. 5*B* and *C*). Wnt7a and PTN upregulation showed similar levels of increased in DCX+ DAPI+ EdU+ cells, but these increases are not significantly high (expression Wnt7a: 21.77 ± 6.81, expression PTN: 22.58 ± 3.63 cells per $mm^2$; ANOVA: $P > 0.05$) (Fig. 5*B* and *C*). In microRNA knockdown conditions, Wnt7a and CCL9 downregulation both showed similar neuroblast densities compared to miR control group (miR Wnt7a: 15.40 ± 3.14, miR CCL9: 12.45 ± 2.10 vs. miR control: 10.45 ± 2.19 cells per $mm^2$; $P > 0.05$) (Fig. 5*B* and *C*). Interestingly, this increase was significantly higher in the PTN knockdown group (28.56 ± 5.65 cells per $mm^2$; ANOVA: $P < 0.01$) (Fig. 5*B* and *C*).

Long-term neurogenesis was assessed based on the density of mature neurons in the peri-infarct cortex. CCL9 upregulation showed a significantly higher density of NeuN+/EdU+ mature neurons compared to expression control animals (expression CCL9: 8.48 ± 0.76 vs. expression

control: 1.67 ± 0.48 cells per $mm^2$; ANOVA: $P<0.0001$) (Fig. 6*A* and *C*) Similarly, Wnt7a upregulation also showed an increase in mature neurons 42 days after stroke (expression Wnt7a: 5.14 ± 0.89; ANOVA: $P<0.01$) (Fig. 6*A* and *C*). The PTN overexpression group, however, did not display an increase in neuronal cells long-term after stroke (expression PTN: 1.13 ± 0.60 cells per $mm^2$; ANOVA: $P>0.05$). microRNA knockdown experiments showed CCL9 downregulation after stroke drastically decreased the number of mature neurons in the peri-infarct cortex (miR CCL9: 3.40 ± 0.61 vs. miR control: 15.29 ± 4.87 cells per $mm^2$; ANOVA: $P<0.05$) (Fig. 6*A* and *B*). This downregulation was also consistent with PTN knockdown (miR PTN: 3.56 ± 1.13 cells per $mm^2$; ANOVA: $P<0.05$) (Fig. 6*A* and *B*). However, Wnt7a knockdown did not produce a significant decrease in NeuN+ EdU+ cells after stroke (miR Wnt7a: 6.52 ± 1.47 cells per $mm^2$; ANOVA: $P>0.05$) (Fig. 6*A* and *B*). Interestingly, expression and microRNA control groups had different levels of NeuN+EdU+ cell densities, suggesting a potential off-target effect of the microRNA itself (expression control: 1.67 ± 0.48 vs. miR control: 15.29 ± 4.87 cells per $mm^2$). These experiments show Wnt7a and CCL9 has a functional role in increasing neurogenesis after stroke by inducing migration of immature neural progenitor cells and promoting the differentiation of neuroblasts into mature neurons.

**Neuroblast-Secreted Factors Mediate Angiogenesis**

To examine whether functional overexpression or knockdown affect stroke-induced angiogenesis, we first examined endothelial cell proliferation, using the co-labeling of endothelial-biomarker cluster of differentiation 31 (CD31), and EdU. We compared angiogenesis at both short-term (14 days) and long-term (42 days) time points after stroke. 14 days after stroke, induced expression of CCL9 slightly increased the density of newly proliferated endothelial cells compared

to stroke expression control group, but this increase was not significant (expression CCL9: 702.60 ± 61.42 vs. expression control: 485.80 ± 65.06 cells per $mm^2$; ANOVA: $P > 0.05$) (Fig. 7*A*). PTN and Wnt7a upregulation both induced proliferation to a comparable level as stroke control expression group (expression PTN group: 599.20 ± 47.53 and expression Wnt7a group: 466.00 ± 102.10 vs expression control group: 485.80 ± 65.06 cells per $mm^2$; ANOVA: $P > 0.05$) (Fig. 7*A*). Wnt7a downregulation drastically decreased the density of new endothelial cells compared to miR control animals (miR Wnt7a: 315.00 ± 66.75 vs. miR control: 701.20 ± 102.70 cells per $mm^2$; ANOVA: $P < 0.01$) (Fig. 7*A*). This significant decrease was also observed in CCL9 knockdown animals (miR CCL9: 469.20 ± 39.81 vs. miR control: 701.20 ± 102.70 cells per $mm^2$; ANOVA: $P < 0.05$) (Fig. 7*A*). Endothelial cell proliferation was not significant in PTN knockdown animals relative to miR control group (597.00 ± 44.09 vs. 701.20 ± 102.70 cells per $mm^2$; ANOVA: $P > 0.05$) (Fig. 7*A*). At 42 days after stroke, increases in endothelial cell proliferation was more apparent in Wnt7a overexpressing animals (expression Wnt7a: 578.00 ± 134.10 vs expression control: 161.50 ± 8.80 cells per $mm^2$; ANOVA: $P < 0.01$) (Fig. 7*A* and *B*). This increase was most significant in CCL9 overexpression cohort (expression CCL9: 1,013.00 ± 53.92 vs expression control: 161.50 ± 8.80 cells per $mm^2$; ANOVA: $P < 0.0001$) (Fig. 7*A* and *B*). PTN overexpression only showed slight increase in endothelial cell proliferation at 42 days after stroke, similar to the short-term effect (368.20 ± 43.03 cells per $mm^2$; ANOVA: $P > 0.05$) (Fig. 7*A* and *B*).

In microRNA knockdown groups, Wnt7a downregulation did not decrease the number of CD31+EdU+ endothelial cells significantly relative to miR control animals (miR Wnt7a: 792.80 ± 86.22 vs miR control: 589.00 ± 76.48 cells per $mm^2$; ANOVA: $P > 0.05$) (Fig. 7*A* and *B*). This is potentially due to the stroke induced downregulation of Wnt7a in neuroblasts, as seen in the microarray analysis (Table 1). CCL9 knockdown, however, drastically decreased the density of

endothelial cells in the peri-infarct cortex (miR CCL9: 166.00 ± 22.62 vs. miR control: 589.00 ± 76.48 cells per $mm^2$; ANOVA: $P<0.01$) (Fig. 7*A* and *B*). Interestingly, PTN knockdown significantly increased the number of endothelial cells proliferated after stroke in the peri-infarct cortex and this increase was higher than the overexpression of PTN (miR PTN: 937.00 ± 89.81 vs. miR control: 589.00 ± 76.48 cells per $mm^2$; ANOVA: $P<0.01$) (Fig. 7*A* and *B*).

Angiogenesis was also evaluated using vessel density based on volume of CD31 expression. Similar to endothelial cell proliferation, Wnt7a, CCL9, and PTN overexpression did not produce significant increases in vessel density in the peri-infarct cortex 14 days after stroke (expression Wnt7a: 482,000 ± 129,727, expression CCL9: 495,800 ± 27,29, and expression PTN: 452,400 ± 46,700 vs. expression Control: 247,600 ± 39,829 $um^3$ per section; ANOVA: $P>0.05$) (Fig. 7*A*). However, Wnt7a knockdown significantly decreased vessel density compared to miR control animals, consistent with the decrease in endothelial cell proliferation at 14 days (miR Wnt7a: 344,000 ± 65,648 vs. miR control: 496,600 ± 37,519 $um^3$ per section; ANOVA: $P<0.05$) (Fig. 7*A*). CCL9 and PTN downregulation did not produce such changes relative to the miR control group (miR CCL9: 383,200 ± 29,047, miR PTN: 513,000 ± 8,972 vs. miR control: 496,600 ± 37,519 $um^3$ per section; ANOVA: $P>0.05$) (Fig. 7*A*). Quantification of vessel density at 42 days after stroke showed significant increases in Wnt7a overexpressing animals (expression Wnt7a: 436,590 ± 93,766 vs. expression control: 199,539 ± 33,533 $um^3$ per section; ANOVA: $P<0.05$) (Fig. 7*A* and *B*). This increase was induced by 3-fold in animals overexpressing CCL9 (expression CCL9: 519,826 ± 38,434 vs. expression control: 199,539 ± 33,533 $um^3$ per section; ANOVA: $P<0.01$) (Fig. 7*A* and *B*). Knockdown of CCL9, contrarily, decreased vessel density, consistent with the significant decrease endothelial cell density observed at 42 days post-stroke (miR CCL9: 135,195 ± 15,203 vs. miR control: 419,054 ± 42,298 $um^3$ per section; ANOVA: $P<0.01$) (Fig. 7*A* and *B*).

Wnt7a knockdown did not impact vessel density compared to miR control animals (522,400 ± 21,846 vs. 419,054 ± 42,298 $um^3$ per section; ANOVA: $P>0.05$) (Fig. 7*A* and *B*). Among all treatment groups, animals injected with PTN overexpression virus showed a decrease in vessel volume and endothelial cell proliferation from 14 to 42 days after stroke. At 14 days, vessel density in animals overexpressing PTN was similar to animals with PTN knockdown and these levels in both cohorts did not differ significantly to their relative control animals (Fig 7*A*). However, at 42 days after stroke, the PTN knockdown group had significantly higher vessel density compared to controls (miR PTN: 661,029 ± 95,813 vs. miR control: 419,054 ± 42,298 $um^3$ per section; ANOVA: $P>0.05$) (Fig. 7*A* and *B*). Furthermore, this increase in vessel density was higher than in the PTN overexpression group (expression PTN: 165,982 ± 14,905 vs. miR PTN: 661,029 ± 95,813 $um^3$ per section) (Fig 7*A*). This trend in induced vessel density in PTN knockdown group at the long-term timepoint was similar to endothelial cell proliferation.

Interestingly, expression and miR control groups showed inconsistent results in both endothelial cell proliferation and vessel density, with the miR control group showing consistently higher values in both short- and long-term time points (endothelial cell proliferation: 14d: 485.80 ± 65.06 vs. 701.20 ± 102.70 cells per $mm^2$, 42d: 161.50 ± 8.80 vs. 589.0 ± 76.48 cells per $mm^2$; vessel density: 14d: 247,600 ± 39,829 $um^3$ per section vs. 496,600 ± 37,519 $um^3$ per section, 42d: 199,539 ± 33,533 vs. 419,054 ± 42,298 $um^3$ per section) (Fig 7*A*). These gain- and loss-of-function data suggest Wnt7a and CCL9 may have larger functional roles than PTN. Regulation of these two genes can significantly impact angiogenesis and neurogenesis after stroke and may potentially mediate neural repair.

**Wnt7a gain-of-function after stroke supports blood-brain-barrier formation**

CNS angiogenesis and blood-brain-barrier (BBB) formation are tightly coupled in development.[39] Endothelial cells are an important member in the neurovascular unit and have a key role in BBB function by regulating the movement of ions, molecules, and cells between the blood and the brain.[40] Wnt7a plays an important functional role in BBB formation and CNS angiogenesis during development.[34] CNS endothelial cells form the BBB are characterized by the formation of tight junctions and the expression of transporters to selectively transport nutrients across the BBB.[39] Wnt7a upregulation after stroke increased angiogenesis both at the short term and long term points (Fig. 7*A* and *B*). To determine whether this angiogenesis is linked to BBB formation, we examined the expression of the BBB endothelial cell-specific glucose transporter glut-1 in the peri-infarct cortex.[41] We found that lentiviral-mediated overexpression of Wnt7a at 42 days after stroke increased the percentage of glut-1 expression by 2-fold compared to expression control group (expression Wnt7a: 53.34 ± 4.135% vs. expression control: 24.32 ± 4.730% per section; Student's *t*-test: $P<0.01$) (Fig 8*A* and *B*). This data supports previous findings that Wnt7a is functionally important for BBB formation and shows that, in addition to promoting CNS angiogenesis and neurogenesis, Wnt7a also improves BBB integrity long-term after stroke.

**CCL9-Mediated Microglia Proliferation**

CCL9 is a signaling chemokine ligand that bind to CCR1 receptors found on perivascular macrophages and microglial cells, the resident CNS parenchymal immune cells.[42] To examine microglia proliferation in CCL9-treated groups, we co-labeled microglia/macrophage-specific biomarker ionized calcium binding adaptor molecule 1 (Iba1) and EdU+ to quantify microglial

density after stroke. Surprisingly, CCL9 overexpression did not significantly induce microglia proliferation (expression CCL9: 420.60 ± 22.87 vs. expression control: 363.50 ± 37.89 cells per $mm^2$; Student's *t*-test, $P>0.05$) (Fig. 9*A* and *B*). However, CCL9 knockdown significantly increased the number of microglia in the peri-infarct cortex at 42 days after stroke (miR CCL9: 418.00 ± 47.39 vs. miR control 242.40 ± 48.82, cells per $mm^2$; Student's *t*-test, $P<0.05$) (Fig. 9*A* and *B*).

**Behavioral Assessment of CCL9 as a Novel Therapeutic Ligand**

An examination of angiogenesis and neurogenesis showed CCL9 modulates both processes after stroke. Currently, there has been little literature relating to a functional role of CCL9 in the brain and, especially, in neural repair. Thus, we set forth to determine whether altering the expression of CCL9 would mediate motor recovery of the injured limb. Gain- and loss-of-function lentivirus driving either the CCL9 or its microRNA-knockdown gene were injected into 2-month-old mice 14 days before photothrombotic stroke. Two behavior tests were used to examine motor improvements after stroke: grid-walk and cylinder test. Animals were examined at 1, 4, and 8 weeks post-stroke and were compared to baseline assessed 1 day before virus injection (Fig 10*A*). In the grid-walk test, all groups demonstrated deficit at 1 week after stroke (Fig 10*B*). CCL9 overexpression group showed improvement at 4 weeks after stroke compared to stroke only group based on decreased in foot faults (expression CCL9: 0.058 ± 0.011 vs. stroke-only control: 0.184 ± 0.031 ratio of foot fault over total steps; ANOVA: $P<0.0001$) (Fig 10*B*). This improvement persisted to 8 weeks after stroke (expression CCL9: 0.065 ± 0.009 vs. stroke-only control: 0.123 ± 0.016 ratio foot fault over total steps; ANOVA: $P<0.05$) (Fig 10*B*). However, despite this significant improvement, CCL9 overexpression animals exhibited no significant differences in

improvement compared to expression control, miR control, and CCL9 knockdown groups. In the cylinder test, we examined motor improvement based on preference use the injured limb to touch the cylinder wall. Each assessment was normalized to baseline. In this task, we found no significant improvement in CCL9 overexpression animals compared to stroke-only control group. All experimental groups experienced deficits that persisted until 8 weeks after stroke. The stroke-only control group showed significant deficit in the injured limb at both 4 weeks and 8 weeks, but not 1 week, after stroke (1 week: -0.459 ± 0.164, $P>0.05$, 4 weeks: -0.645 ± 0.132, $P<0.01$, 8 weeks: -0.601 ± 0.140; $P<0.05$) (Fig 10*B*). CCL9 can significantly modulate neurogenesis and angiogenesis after stroke. However, these behavior tests suggest those cellular changes mediated by CCL9 may not be sufficient for improvement from deficits.

## Discussion

Stroke induces neurogenesis and angiogenesis in the tissue adjacent to the ischemic core, forming a unique neurovascular niche with capacity for regeneration.[21] After cortical ischemic injury, SVZ-derived neuroblasts migrate along angiogenic blood vessels and differentiate in the regions adjacent to the infarct.[21,43,44] However, the specific signals involved in this stroke-induced neuroblast-vascular association is largely unknown. Using microarray and bioinformatic analysis, we identified a list of differentially regulated ligand-receptor pairs derived from neuroblasts and endothelial cells in the neurovascular niche. From this list, we investigated the functional properties of three of these ligands in mediating neurogenesis and angiogenesis. These ligands were CCL9, Wnt7a, and PTN.

A set of gain- and loss-of-function studies using lentiviral-mediated overexpression and knock-down demonstrated these signaling ligands can induce neurogenesis and angiogenesis in the short-term and, more significantly, in the long-term recovery time points after stroke. Gain of Wnt7a function after ischemia increased the density of mature neurons, endothelial cells, and overall vessel volume in the long-term but not short-term period after stroke. Wnt7a expression is vital for CNS vascular formation during development; Wnt7a inhibition leads to CNS-specific vessel defects.[34] The pro-angiogenic property of Wnt7a found in this study supports its relevance in CNS angiogenesis, and more importantly its functional role in promoting angiogenesis after ischemic injury in an adult mouse model. Further, we demonstrated Wnt7a increase the expression of a BBB endothelial cell-specific glucose transporter, indicating the possibility that in addition to promoting angiogenesis it also drives barrier formation in the newly formed vessels. This is particularly important as the movement of toxins and nutrients between the blood and the brain are tightly controlled by the expression of specific transporters in the BBB.[40,45] As ischemia

progresses, the BBB becomes increasingly permeable, leaving brain tissue vulnerable to a plethora of inflammatory responses and toxins that further aggravate injury.[46,47] Formation of the BBB in angiogenic vessels would facilitate the influx and efflux of nutrients and maintain CNS homeostasis and proper functions of remaining and newly differentiated neurons. Gain-of Wnt7a function increased neurogenesis in the long-term period after stroke. This result aligns with previous studies which have demonstrated the neurogenic property of Wnt7a in the naïve mouse brain. Extensive studies have shown Wnt7a stimulates proliferation and differentiation of embryonic and neonatal neural progenitor cells derived from mouse brains.[48,49] In the adult mouse, Wnt7a regulates multiple steps of neurogenesis and promotes cell renewal and cycle progression.[35,50] The Wnt7a/canonical signaling pathway is critical in these angiogenic and neurogenic changes. This pathway begins with the activation of the Frizzled receptor followed by stabilization of β-catenin, activating downstream targets.[51] Blockade of β-catenin leads to vascular malformation and loss of BBB-specific transporters during development.[34] β-catenin signaling also promotes neural stem cell self-renewal, neural progenitor cell progression and differentiation, and synaptic input in the adult SVZ and hippocampus.[35,50] Based on these findings, Wnt7a-induced angiogenesis and neurogenesis after-stroke may be regulated by canonical signaling through β-catenin and its downstream effectors. Targeting the molecules downstream of this pathway may be crucial to the neurovascular regenerative process. Specifically, Cyclin D1, a downstream target of β-catenin, regulates early steps of neurogenesis by promoting neural progenitor proliferation; and, in later stages of neurogenesis, activation of neurogenin 2 leads to neuronal differentiation and maturation.[35,52] Furthermore, Wnt7a promotes hippocampal synapse formation and axonal guidance during critical developmental stages; both of these processes are important for the function and integration of new neurons and can lead to functional recovery.[53–58] Future

experiments could focus on determining whether Wnt7a expression alters synaptogenesis and axonal remodeling of existing and newly differentiated neurons after stroke after stroke to better characterize the functionality of these neurons in the neurovascular niche. Further, β-catenin and its downstream targets such as Cyclin D1 and neurogenin after stroke should be examined to see whether activating the signaling pathway directly can further increase the angiogenic and neurogenic response after stroke and whether this can increase synaptic formation and integration of newly differentiated neurons into cortical network.

PTN is a heparin-binding protein that stimulates mitogenesis, angiogenesis, and neurite and glial process guidance during embryogenesis and early development.[33] The PTN gene is predominantly expressed in cortical neurons in adult mouse brains.[59] After acute ischemia, up-regulation of PTN have been discovered in astrocytes, macrophages, and endothelial cells.[33] Adding to that discovery, our microarray data showed increased PTN expression in SVZ-derived neuroblasts in the peri-infarct cortex. This is consistent with previous findings which have found increased PTN expression after injury and during repair in the brain.[28] Other findings have shown PTN secretion increases tumor angiogenesis and the formation of new blood vessels after cerebral ischemia.[60,61] In this study, PTN overexpression increased endothelial cell proliferation and vessel density increased slightly at 14 days but returned to baseline at 42 days after stroke. Interestingly, PTN knockdown significantly increased both endothelial cell and vessel densities at 42 days after stroke. This result conflicts with previous findings which showed PTN secretion stimulates endothelial cell proliferation and angiogenesis in human glioma.[29,60] Similar to angiogenesis, PTN overexpression resulted in similar densities of neuroblasts and mature neurons compared control animals at 14 and 42 days after stroke. However, PTN knockdown induced a greater number of neuroblast proliferation, but the number of mature neurons drastically decreased to baseline at 42

days. These data suggest that PTN expression after stroke may potentially inhibit neuronal proliferation, but this inhibition is released with PTN knockdown and other secreted factors may be necessary to regulate later steps of neurogenesis to promote differentiation into mature neurons. This implies that PTN may have an inhibitory role in later stages of post-stroke neurogenesis. Since stroke-induced neuroblast migration is linked to angiogenesis in the peri-infarct cortex, the significant increase in long-term angiogenesis with PTN knockdown is perhaps due to growth factors and other signaling ligands secreted by the increase in neuroblast density found in the acute period after stroke.[43] PTN signals through a transmembrane receptor protein tyrosine phosphatase, RPTPβ/ζ, whose activity is inactivated upon PTN binding, leading to persistent phosphorylation of a variety of substrates.[60] One of these substrates is β-catenin, a downstream protein also activated by Wnt7a.[62] Future experiments could combine PTN knockdown and Wnt7a up-regulation based on the results of this study and examine whether Wnt7a upregulation can increase the differentiation of neuroblasts that are initially induced by PTN knockdown.

CCL9 up-regulation in the peri-infarct cortex after stroke increased both neurogenesis and angiogenesis long-term. CCL9 expression increased neuroblast proliferation and differentiation into neurons and endothelial cell proliferation and vascular density. However, this significance was only observed at 42 days after stroke, suggesting this regenerative effect may take longer than the 14-day period. CCL9 down-regulation, contrarily, decreased these effects. These data in tissue repair suggested CCL9 might serve as a therapeutic target for functional recovery. However, behavioral assessment of motor movements in mice with CCL9 up-regulation did not show consistent improvement across the grid-walk and cylinder tests. CCL9 overexpression animals showed improvements at 4 and 8 weeks after stroke compared to stroke-only control animals in the grid-walk test; but this improvement was not significantly different compared to expression

virus control, CCL9 microRNA knockdown, or microRNA knockdown virus control animals. Furthermore, there was no significant improvements in CCL9 overexpressing animals relative to stroke-only animals in the cylinder task. Together, these data show CCL9 has a regenerative effect on neural repair, but these effects are not sufficient to generate functional recovery. CCL9, normally expressed in macrophages, signals through CCR1 and induces tumor angiogenesis through myeloid progenitor cell recruitment.[24,26,63] Microglia cells are the resident immune cells in the brain.[64] Upon examination of microglia density after stroke, there was no apparent increase in CCL9 overexpression groups compared to control animals. Interestingly, CCL9 knockdown produced moderated increase compared to microRNA knockdown control animals. However, the densities between CCL9 overexpression and knockdown were similar, suggesting CCL9 does not significantly affect microglia recruitment after stroke. This is contrary to findings that show CCL9 induces tumor angiogenesis through macrophage recruitment.[65] One possible explanation for the angiogenic effect in our studies is that CCL9-induced angiogenesis in the stroke is not mediated through microglia. CCL9 can potentially target the CCR1 receptor on the endothelial cells directly to stimulate proliferation and vessel growth. Additionally, inflammatory response following ischemia induces the release of a variety of chemokines and cytokines that activates microglia and recruit peripheral infiltrating macrophages.[66] Therefore, mediating CCL9 expression alone may not be sufficient to drastically alter microglial activation, while other chemokines may play a larger role in the inflammatory response. CCL3, a macrophage inflammatory protein that also signals through CCR1, is also induced in focal cerebral ischemia; its induction exacerbates injury that is correlated to the recruitment of inflammatory immune cells.[67,68] Other studies have shown human colon cancer cells secrete CCL9 and blocking CCR1 decreased myeloid cell accumulation.[69] Based on these findings, blockade of the CCR1 receptor after stroke may be a better target to examine

and enhance motor recovery and microglial proliferation. Using CCR1 antagonists can potentially have an enhanced effect on tissue repair and functional recovery, especially given that CCL9 expression did not change behavioral outcomes.

In this study, we discovered a set of gene products isolated from the neurovascular niche and defined the functional effect of a small set of those genes on both tissue regeneration and behavioral recovery. The workflow developed in this study demonstrated stroke-responsive neuroblast-derived ligands, Wnt7a, CCL9, and PTN, can mediate post-stroke neurogenesis and angiogenesis. One limitation of this selection approach is that gene products were chosen based on results from microarray analysis, which needs to be further validated and does not precisely describe post-translational modifications that can regulate the activity of signaling ligands and their interaction with receptors.[70,71] A more rigorous validation of the microarray data using in situ hybridization chain reaction can demonstrate the precise location within the neuroblast of these signaling molecules and their respective receptors on the endothelial cells. Nevertheless, we have established a set of gene products that are at least partially involved in the interaction between neuroblasts and angiogenic vessels in the stroke neurovascular niche. Further explorations of this dataset can lead to a better understanding of the precise mechanisms involved in this cellular interaction and can potentially lead to promising therapeutic targets for clinical recovery.

**Figure 1**. **Microarray and bioinformatics analysis of cellular interactions in the peri-infarct cortex.** (*A*) Confocal micrograph of DCX+ neuroblasts migrating to the infarct in MCAo stroke tissue. (*B*) Schematic of the regenerating Neurovascular Interactome. Stroke-responsive neuroblasts and endothelial cells from the peri-infarct and contralateral cortex and olfactory bulb are isolated 7 days after a MCAo stroke. (Scale Bar: 1000µm).

**A.**

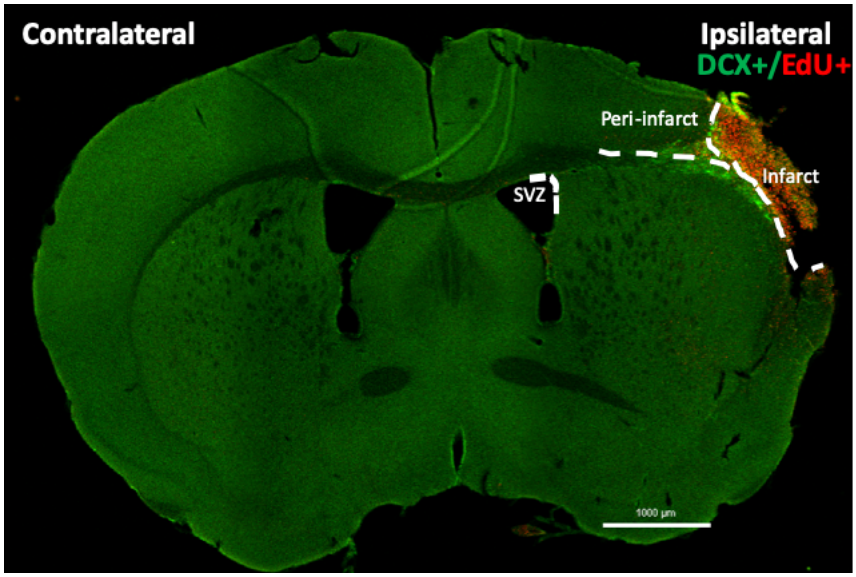


**B.**

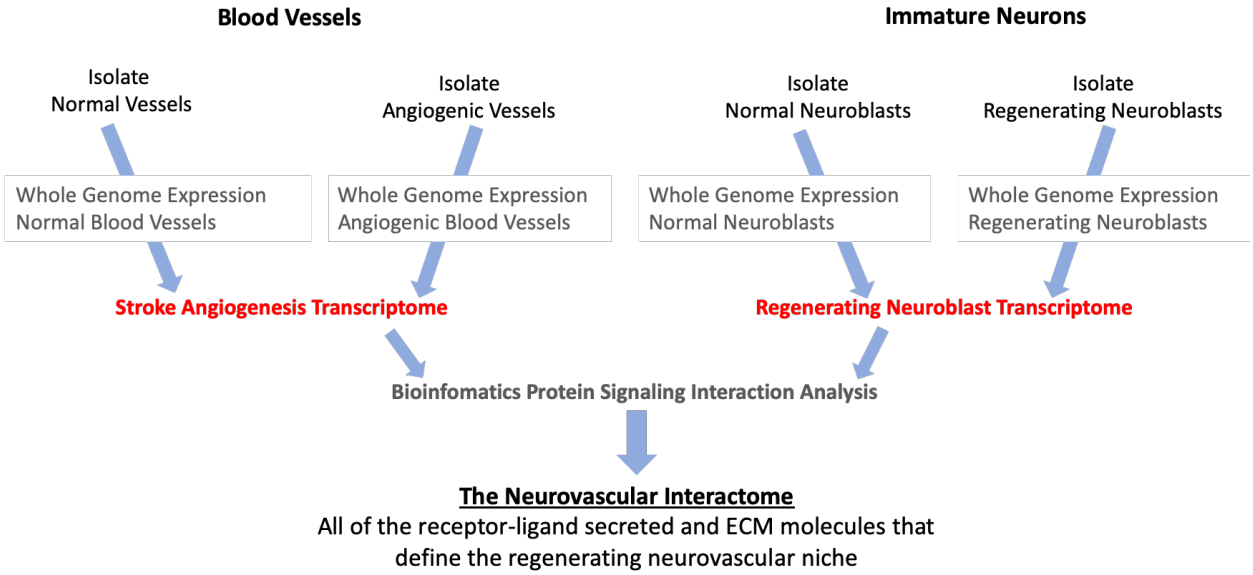

**Figure 2. Ligand expression in naïve and stroke animals.** (*A*) Confocal micrograph of PTN expression in NeuN+ cells in the cortex of a 2-month-old naïve animal. (Scale bar: 50µm). (*B*) CCL9 expression adjacent to CD31+ vessels in the peri-infarct cortex 7 days after stroke. (Scale bar: 50µm). (*C*) Confocal micrograph of Wnt7a expression found in NeuN+ cells in the cortex and DCX+ cells in the olfactory bulb of a naïve animal, but not in DCX+ cells in the SVZ 7 days after stroke. (Scale bar: 50µm).

**A.**

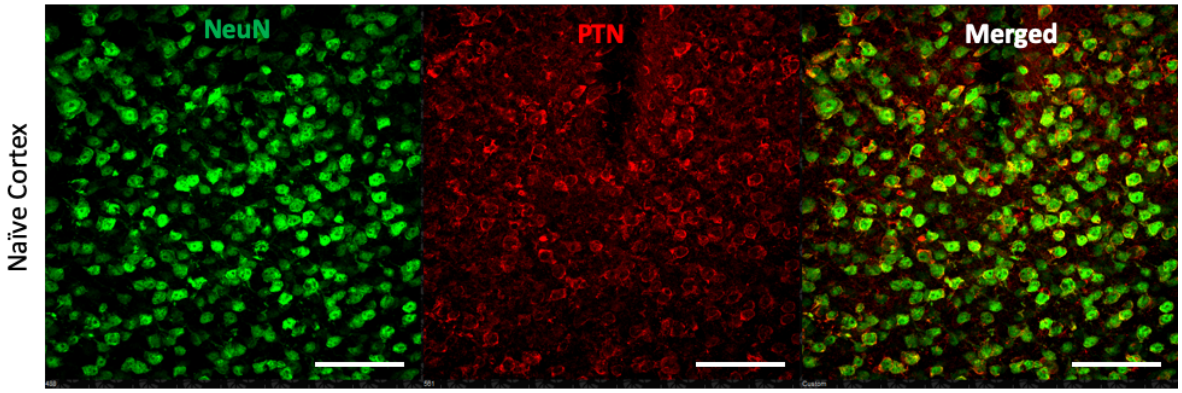


**B.**

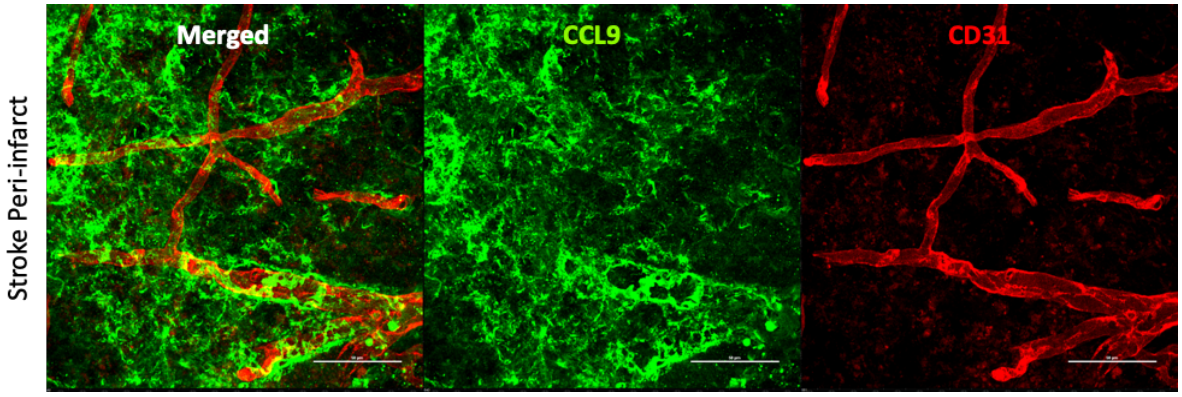

C.

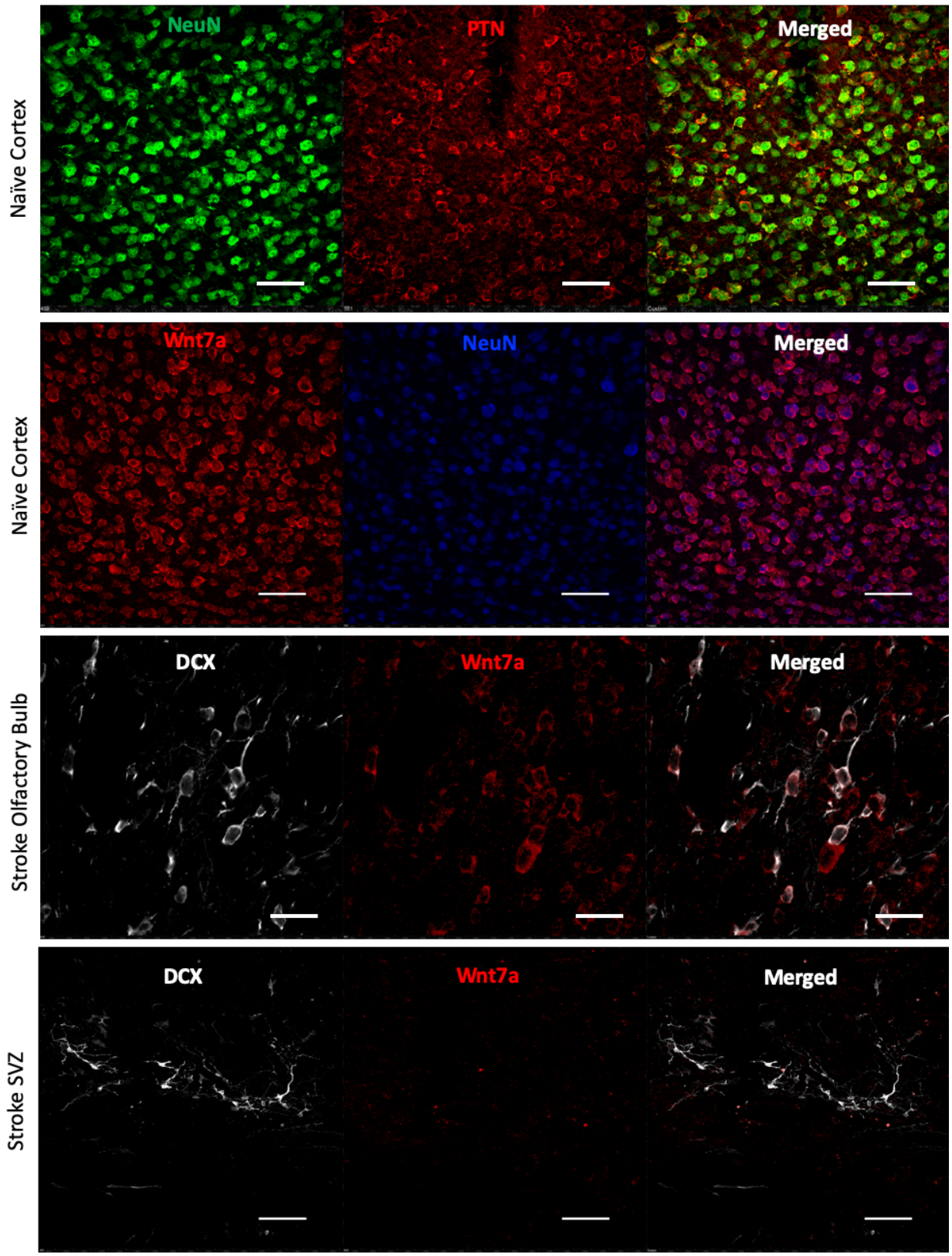
Naïve Cortex
NeuN
PTN
Merged
Naïve Cortex
Wnt7a
NeuN
Merged
Stroke Olfactory Bulb
DCX
Wnt7a
Merged
Stroke SVZ
DCX
Wnt7a
Merged

**Figure 3. Gain- and loss-of-function virus expression after stroke.** (*A*) Low magnification confocal micrograph of viral expression in whole brain coronal section 14 days after photothrombotic stroke. Lentiviruses are injected into the medial and lateral cortex of the animal 14 days before stroke. (Scale bar: 1,000µm). (*B*) Confocal micrograph of lentiviral expression indicated by BFP+ cells in the motor cortex 14 days after injection. (Scale bar: 100µm). (*C*) Confocal micrographs of transduced cells in the per-infarct cortex 14 days after injection. Arrowheads: BFP+ NeuN+ and BFP+ GFAP+ cells (Scale bar: 50µm).

**A.**

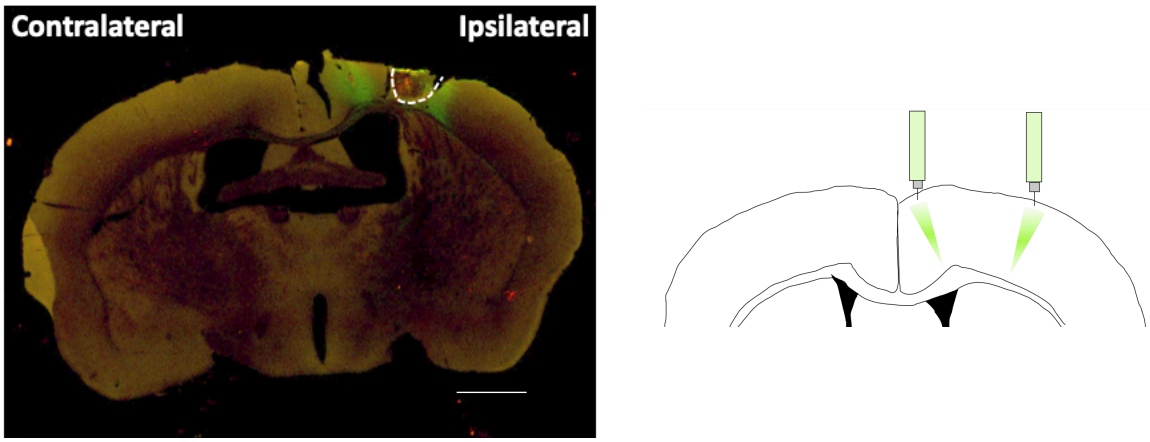


**B.**

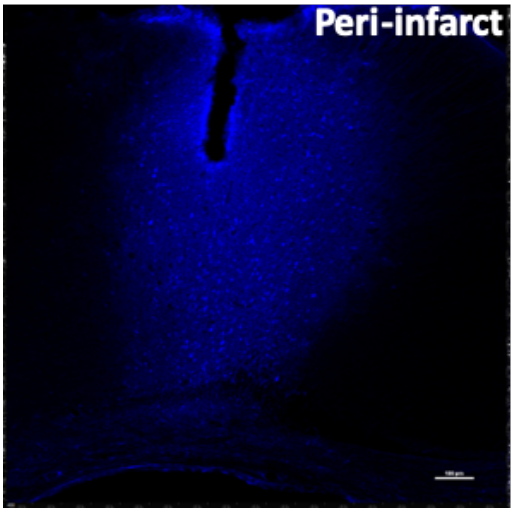

**C.**

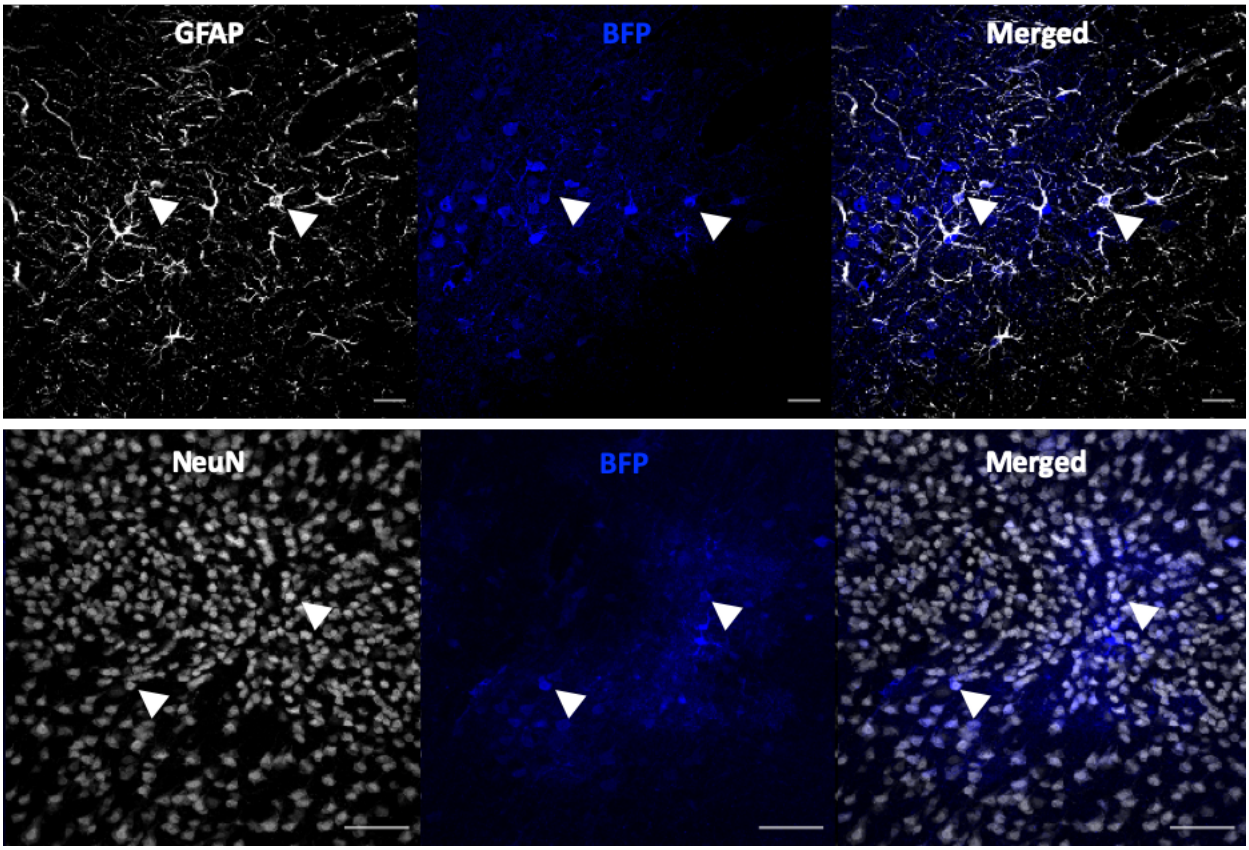

**Figure 4. Post-stroke neurogenesis in Ascl1-CreERT2::tdTomato transgenic line.** (*A, B*) Expression of Ascl1-CreERT2::tdTomato cells at 3 days and 10 days after stroke. Tamoxifen was administered once per day from for 5 days after stroke. Confocal micrographs of migration of DCX+ tdTomato+ cells in the ipsilateral cortex at 3 days (*A*) and 10 days (*B*) after stroke. (Scale bar: 100µm)

**A.**

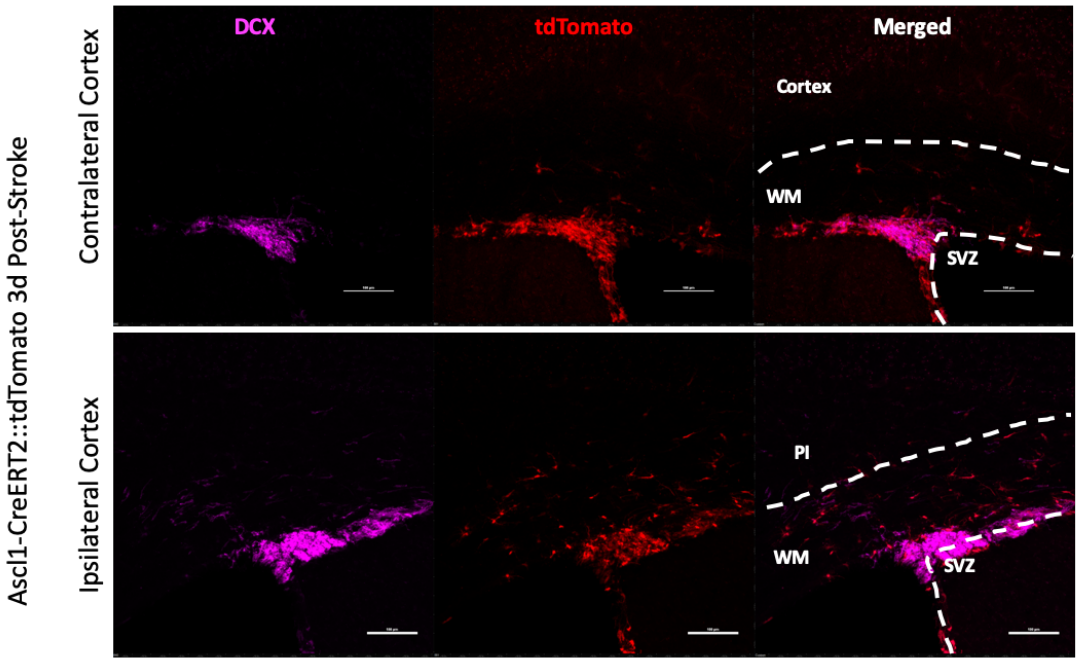


**B.**

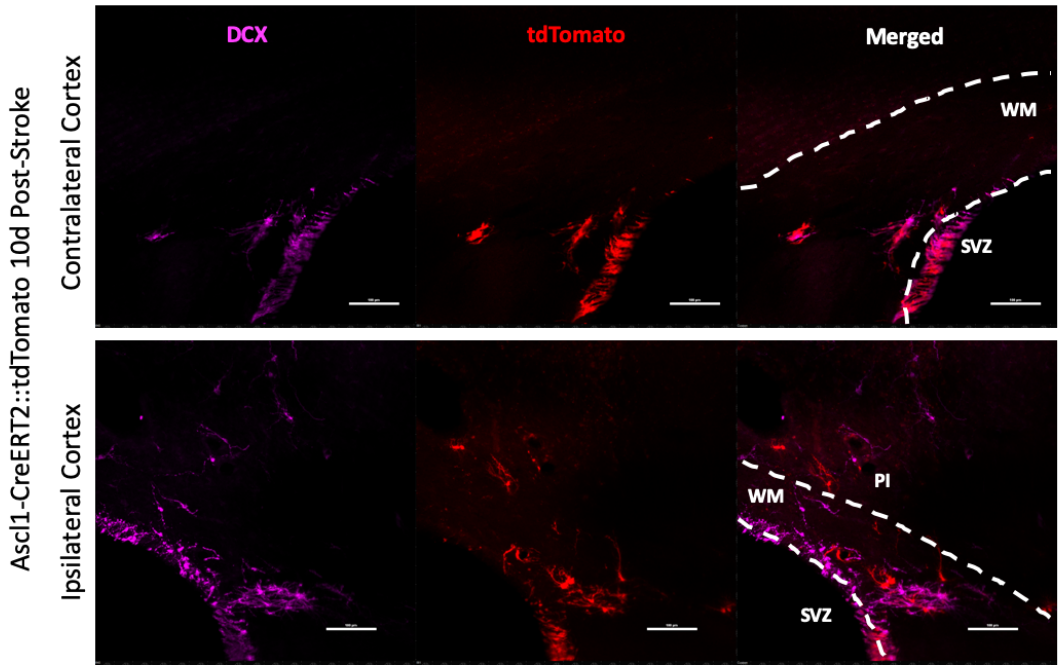

**Figure 5. Short-term post-stroke neurogenesis.** (*A*) Low magnification confocal micrograph of a coronal section of a photothrombotic stroked brain. Expression of DCX+ cells in the subventricular zone (SVZ), white matter (WM), and the peri-infarct is shown in higher magnification. (Scale bar: 1,000µm in lower magnification, 100µm in higher magnification). (*B*) Quantification of DCX+ DAPI+ EdU+ neuroblast density 14 days after stroke. For all group comparisons, One-Way ANOVA, n= 5 for all groups, ** $P<0.01$. (*C*) Confocal micrographs of gain-of-function and loss-of-function CCL9, Wnt7a, and PTN treated animals. Arrowheads: Co-labeled DCX+ DAPI+ EdU+ indicate stroke-induced neuroblast proliferation. (Scale bar: 30µm).

**A.**

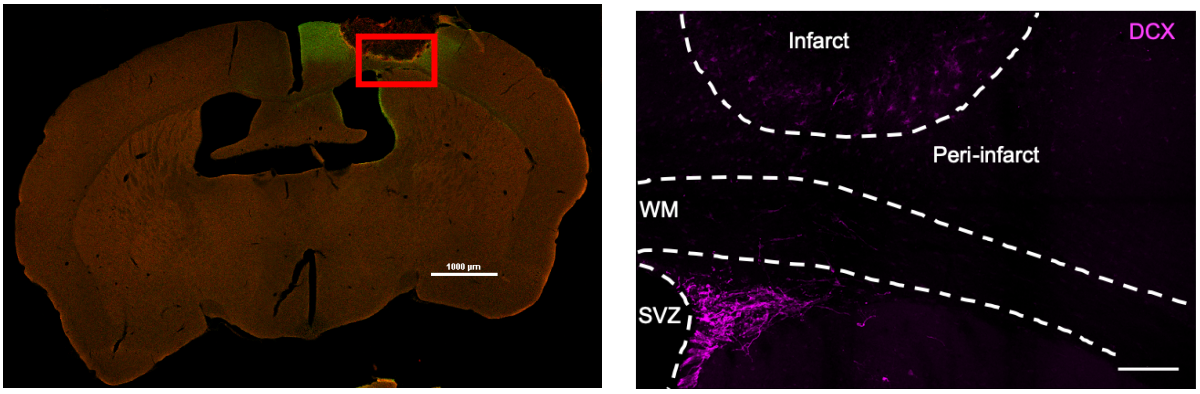


**B.**

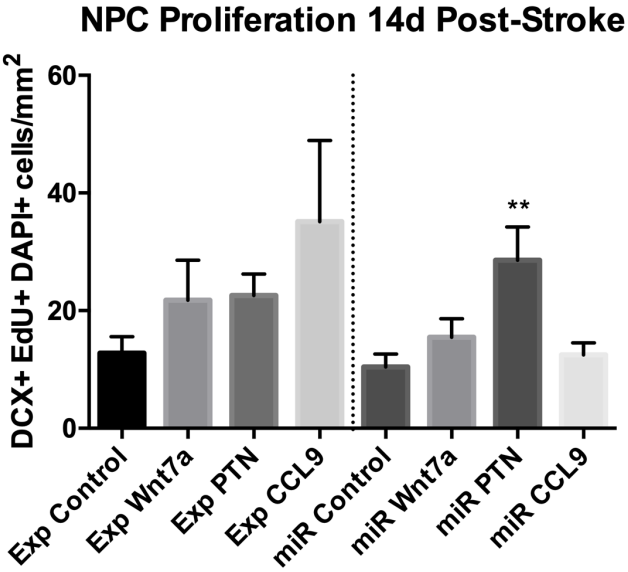

**C.**

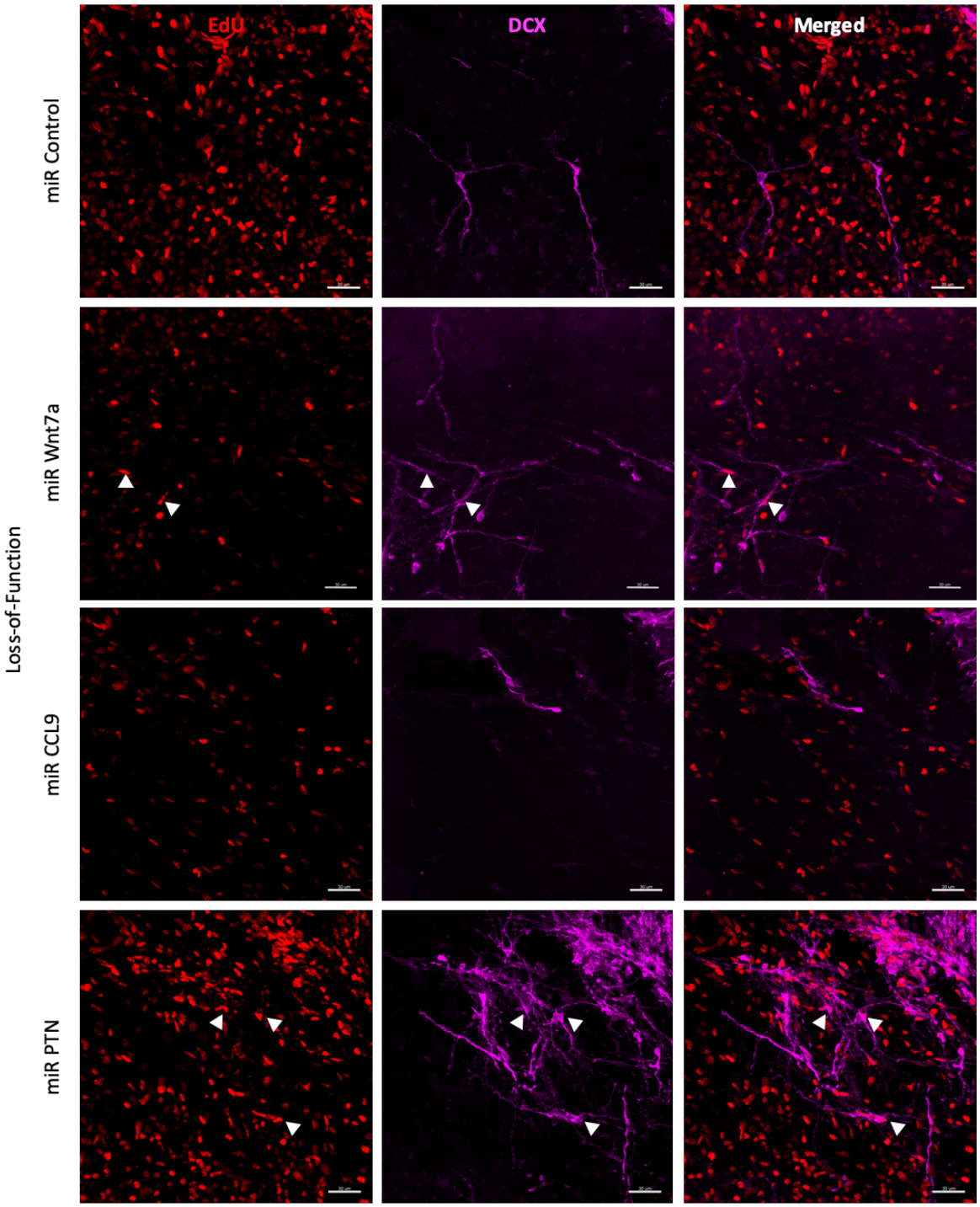
EdU
DCX
Merged
Loss-of-Function
miR Control
miR Wnt7a
miR CCL9
miR PTN

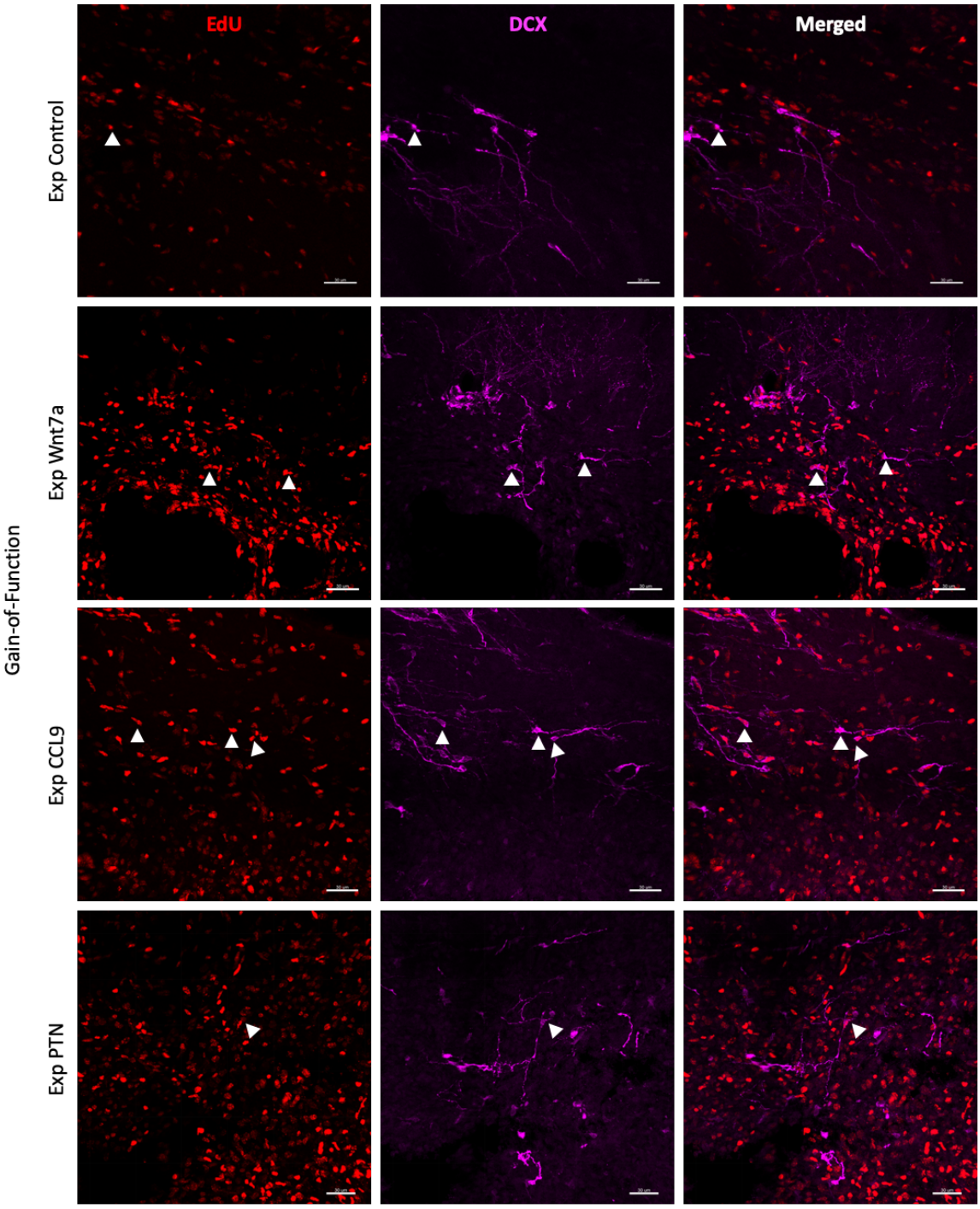
EdU
DCX
Merged
Gain-of-Function
Exp Control
Exp Wnt7a
Exp CCL9
Exp PTN

**Figure 6. Long-term post-stroke neurogenesis.** (*A)* Quantification of NeuN+ EdU+ cell density 42 days after stroke. (*B*) Confocal micrographs of mature neurons in the peri-infarct cortex in gain- and loss-of-function groups. Arrowheads: NeuN+ EdU+ cells. One-way ANOVA, n=5 for all groups, * $P<0.05$, ** $P<0.01$, **** $P<0.0001$. (Scale bar: 12.5μm).

**A.**

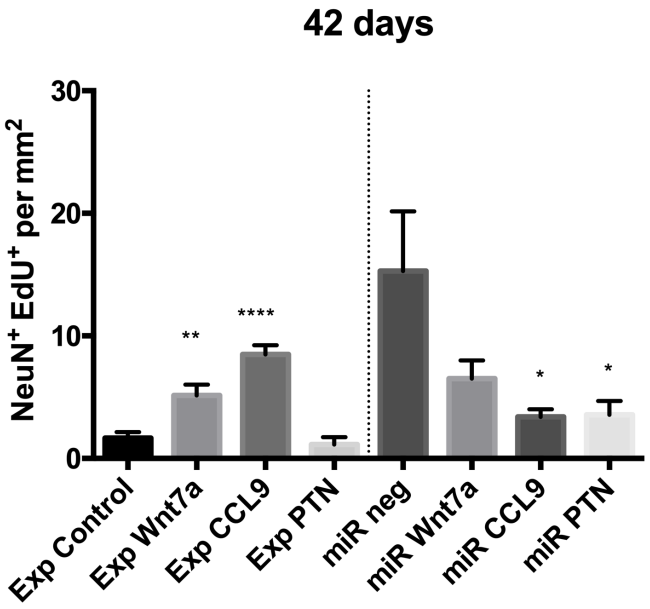

**B.**

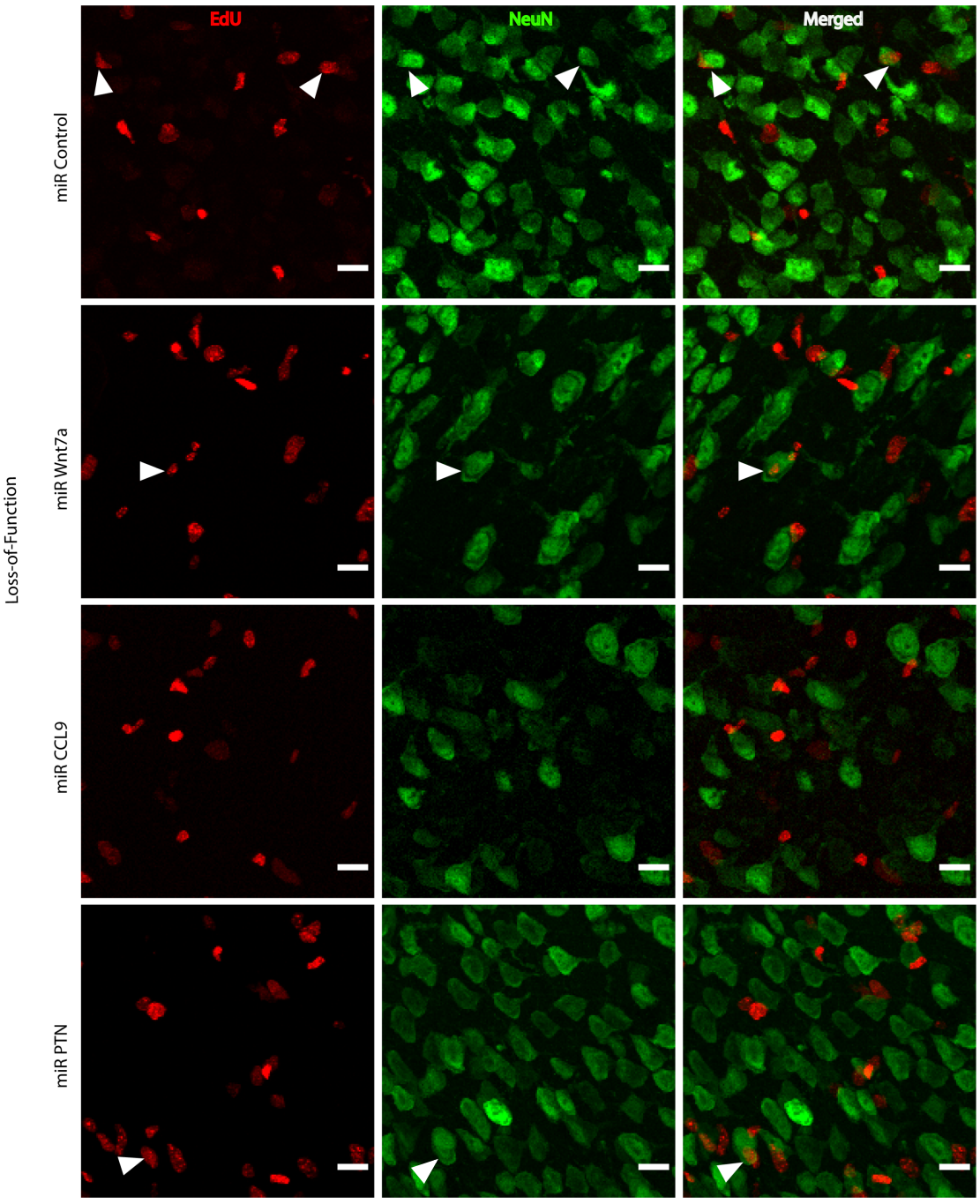
EdU
NeuN
Merged
miR Control
miR Wnt7a
miR CCL9
miR PTN
Loss-of-Function

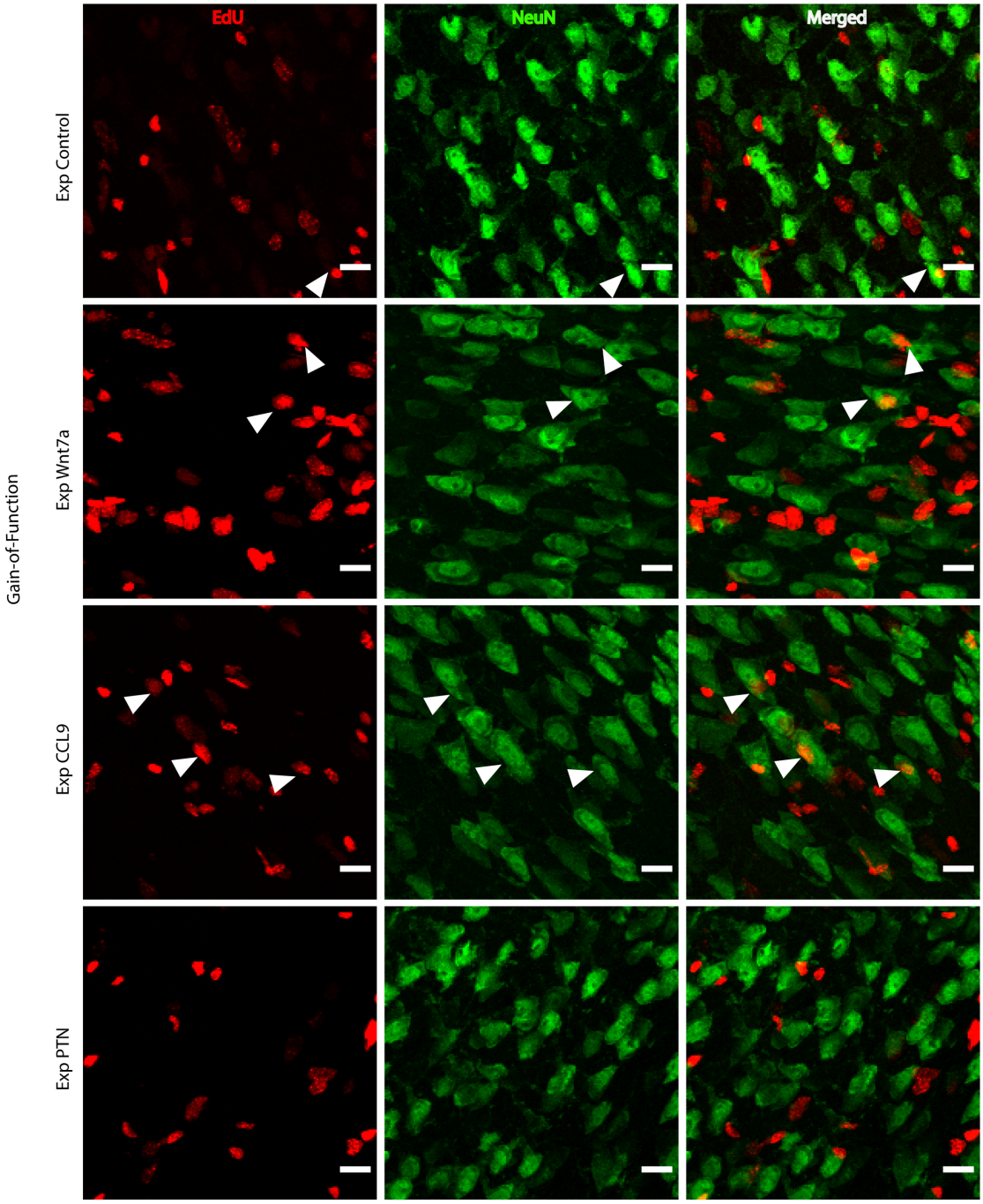
EdU
NeuN
Merged
Exp Control
Exp Wnt7a
Exp CCL9
Exp PTN
Gain-of-Function

**Figure 7. Post-Stroke angiogenesis.** (*A*) Quantification of CD31+ EdU+ endothelial cells and CD31+ vessel density at 14 and 42 days after stroke. For all group comparisons, One-Way ANOVA, n=5 for all groups, * $P<0.05$, ** $P<0.01$, **** $P<0.0001$. (*B*) Confocal micrographs of angiogenesis at 42 days after stroke. Arrowheads: co-labeled CD31+ EdU+ endothelial cells. (Bar: 50μm).

**A.**

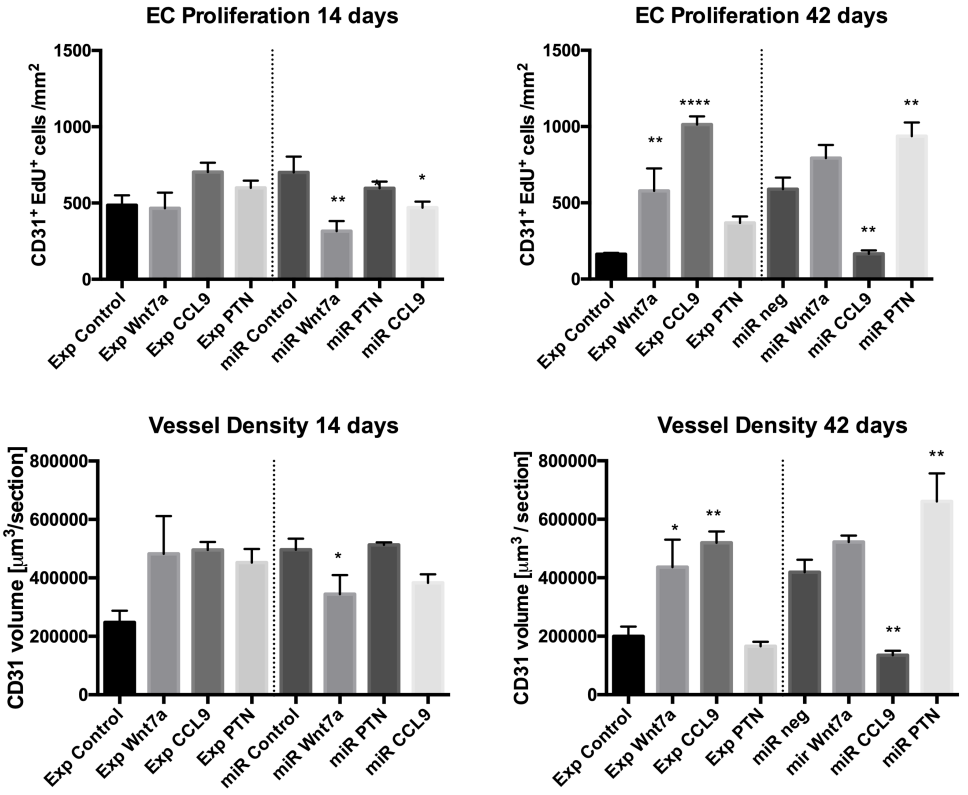


**B.**

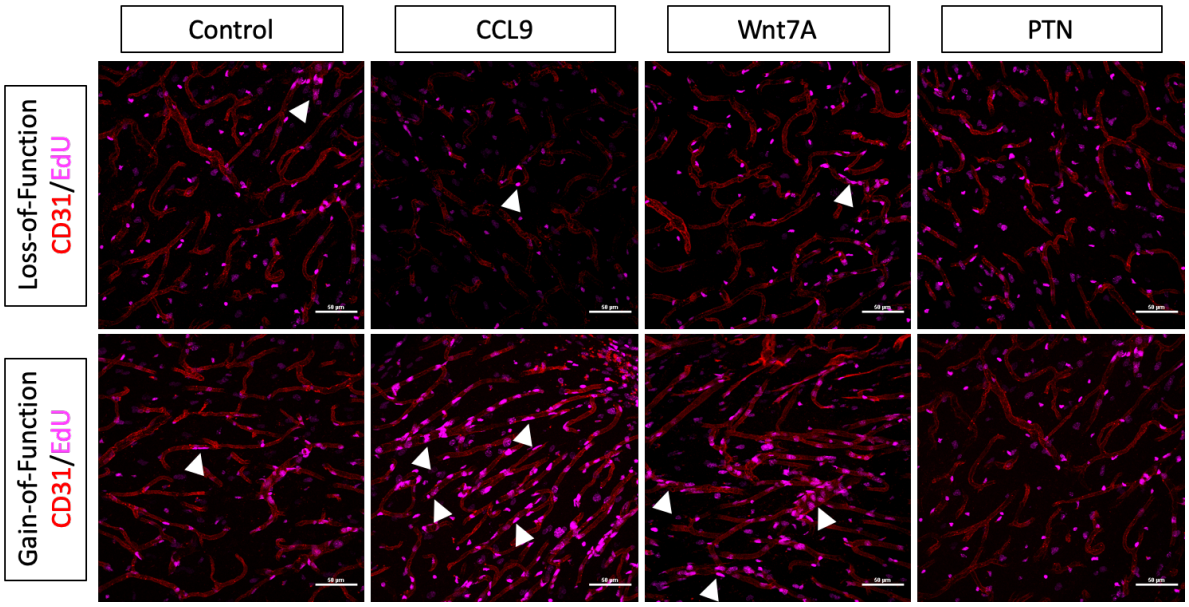

**Figure 8. Wnt7a increases blood-brain-barrier formation.** (*A*) Quantification of Glut1 expression in Wnt7a overexpression and expression control animals 42 days after stroke. Student's *t*-test, n=5 for all groups, ***P*<0.01. (*B*) Confocal micrograph of Glut-1 expression in Wnt7a gain-of-function and control mice. (Bar: 50μm).

**A.**


**B.**

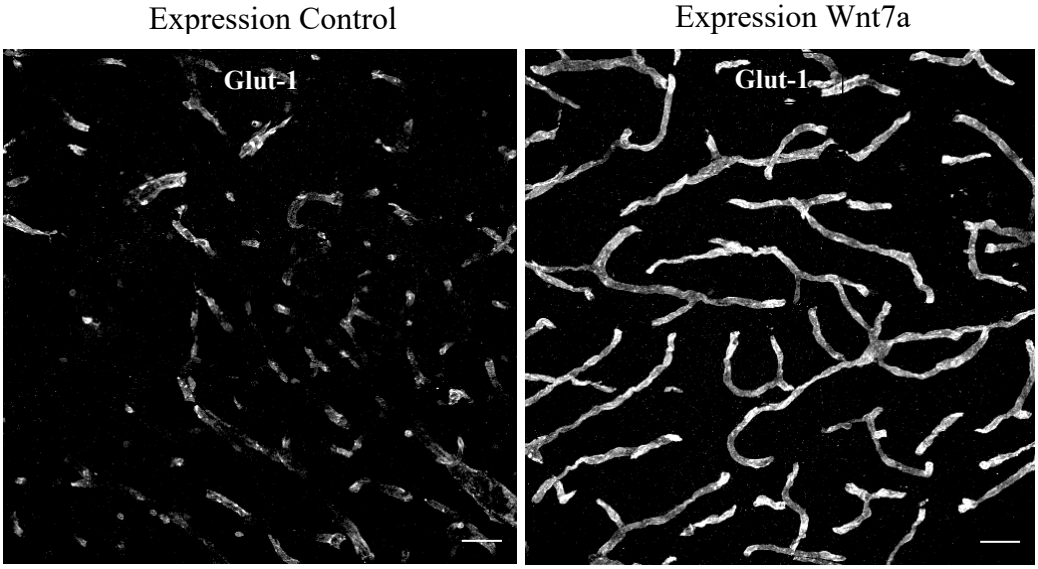

**Figure 9. CCL9-Induced Microglial Activation.** (*A*) Quantification of Iba1+ EdU+ cell density in the peri-infarct cortex 42 days after stroke. Student's t-test, n= 5 for all groups, **P*<0.05. (*B*) Confocal micrographs of Iba1+ EdU+ microglia assessed in the peri-infarct cortex 42 days after stroke. (Scale bar: 50μm).

**A.**

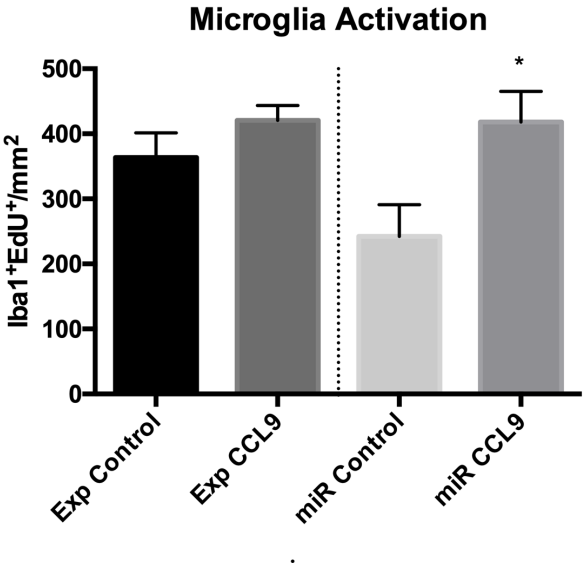

**B.**

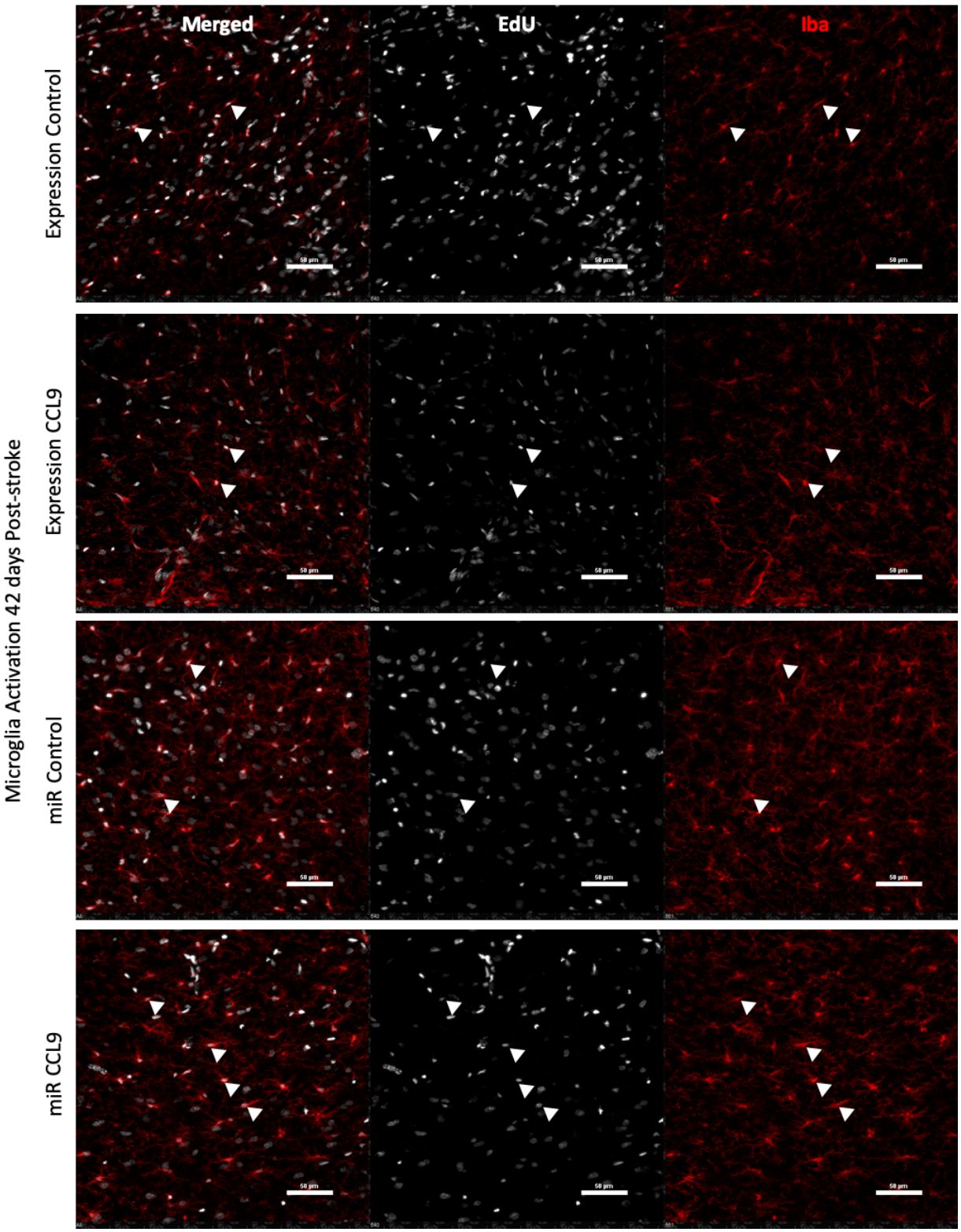
Merged
EdU
Iba
Expression Control
Expression CCL9
miR Control
miR CCL9
Microglia Activation 42 days Post-stroke

**Figure 10. Behavior assessment of CCL9 gain- and loss-of-function.** (*A*) Gain-of-function and loss-of-function viruses were injected 2 weeks before stroke. Grid walk and cylinder tasks were assessed 1 day before virus injection to establish baseline and at 1 week, 4 weeks, and 8 weeks after stroke. (*B*) Quantification of foot faults in grid-walk test. Two-way ANOVA, **P*<0.05, *****P*<0.0001. (*C*) Assessment of preference for injured over uninjured limb use. Two-way ANOVA, **P*<0.05, ***P*<0.01, stroke-only vs. naïve animals, n=10 for all groups.

**A.**

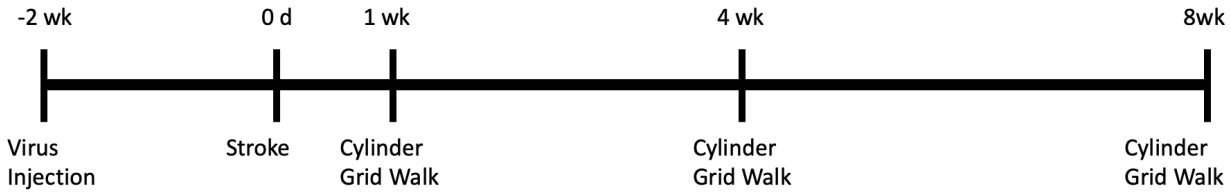


**B.**

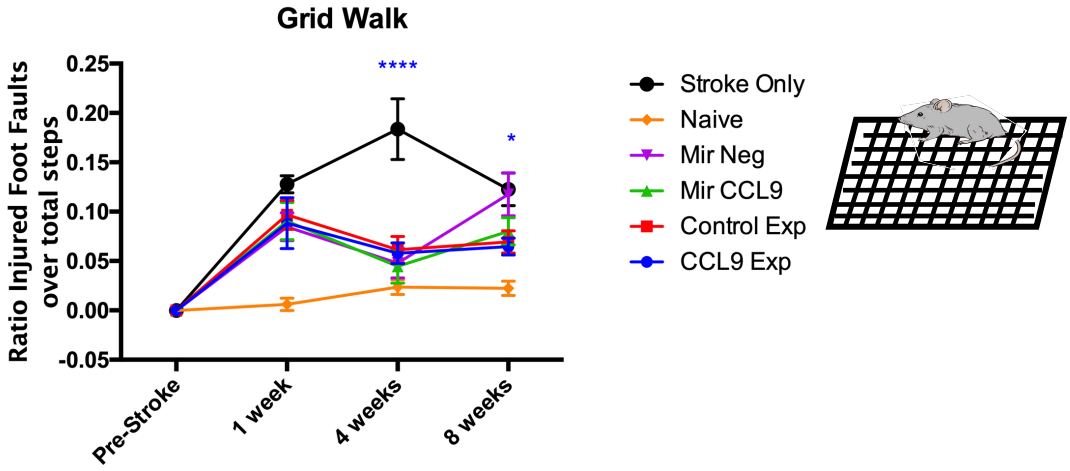


**C.**

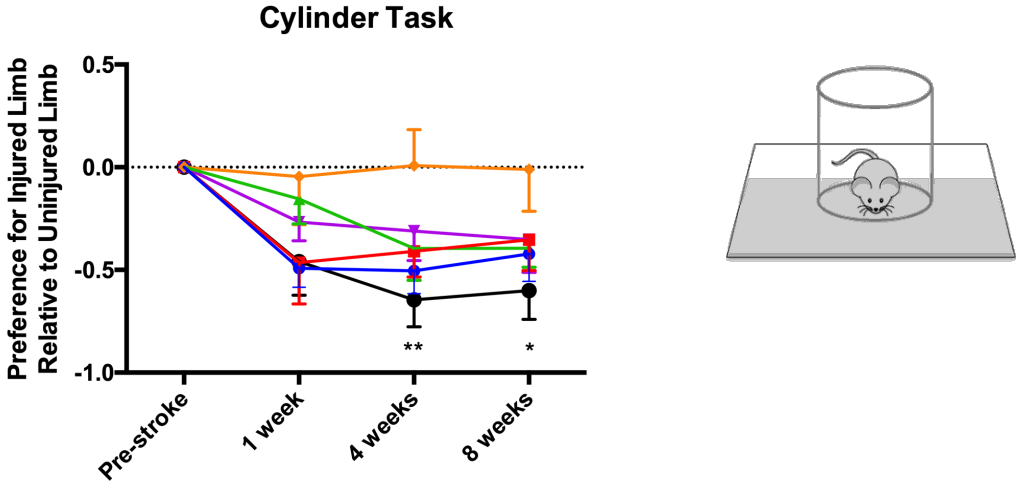

**Table 1. Stroke-responsive neuroblast-derived ligands.**

| Ligand | Receptor | Ligand Expression Fold Change | Location | Type |
|---|---|---|---|---|
| **CCL9** | CCR1 | ↑ 3.040 | Extracelluar Space | Chemokine |
| **Wnt7a** | Frizzled 2/7 | ↓ 0.591 | Extracelluar Space | Growth factor |
| **PTN** | RPTPβ/ζ | ↓ 0.330 | Extracellular Space | Growth factor |

**References**


1. Benjamin, E. J. *et al. Heart disease and stroke statistics - 2018 update: A report from the American Heart Association*. *Circulation* **137**, (2018).
2. Types of Stroke. *Center for Disease Control* (2018). Available at: https://www.cdc.gov/stroke/types_of_stroke.htm. (Accessed: 8th June 2019)
3. Ischemic Stroke Treatment. *American Stroke Association* (2018). Available at: https://www.strokeassociation.org/STROKEORG/AboutStroke/About-Stroke_UCM_308529_SubHomePage.jsp%0D%0A. (Accessed: 8th June 2019)
4. Ramos-Cabrer, P., Campos, F., Sobrino, T. & Castillo, J. Targeting the ischemic penumbra. *Stroke* **42**, 7–11 (2011).
5. Gauberti, M., De Lizarrondo, S. M. & Vivien, D. The "inflammatory penumbra" in ischemic stroke: From clinical data to experimental evidence. *Eur. Stroke J.* **1**, 20–27 (2016).
6. Carmichael, S. T. Cellular and molecular mechanisms of neural repair after stroke: Making waves. *Ann. Neurol.* **59**, 735–742 (2006).
7. Krupinski, J., Kaluza, J., Kumar, P., Kumar, S. & Wang, J. M. Role of angiogenesis in patients with cerebral ischemic stroke. *Stroke* **25**, 1794–1798 (1994).
8. Angels Font, M., Arboix, A. & Krupinski, J. Angiogenesis, Neurogenesis and Neuroplasticity in Ischemic Stroke. *Curr. Cardiol. Rev.* **6**, 238–244 (2010).
9. Gage FH. Mammalian neural stem cells. *Science (80-. ).* **287**, 1433–1438 (2000).
10. Jin, K. *et al.* Evidence for stroke-induced neurogenesis in the human brain. *Proc. Natl. Acad. Sci.* **103**, 13198–13202 (2006).
11. Jin, K. *et al.* Neurogenesis in dentate subgranular zone and rostral subventricular zone

after focal cerebral ischemia in the rat. *Proc. Natl. Acad. Sci.* **98**, 4710–4715 (2001).

12. Gonçalves, J. T., Schafer, S. T. & Gage, F. H. Adult Neurogenesis in the Hippocampus: From Stem Cells to Behavior. *Cell* **167**, 897–914 (2016).
13. Kernie, S. G. & Parent, J. M. Forebrain neurogenesis after focal Ischemic and traumatic brain injury. *Neurobiol. Dis.* **37**, 267–274 (2010).
14. Curtis, M. A. *et al.* Human neuroblasts migrate to the olfactory bulb via a lateral ventricular extension. *Science (80-. ).* (2007). doi:10.1126/science.1136281
15. Fujioka, T., Kaneko, N. & Sawamoto, K. Blood vessels as a scaffold for neuronal migration. *Neurochem. Int.* **126**, 69–73 (2019).
16. Arvidsson, A., Collin, T., Kirk, D., Kokaia, Z. & O, L. Neuronal replacement from endogenous precursors in the adult. *Nat Med* **9**, 548–553 (2003).
17. Parent, J. M., Vexler, Z. S., Gong, C., Derugin, N. & Ferriero, D. M. Rat forebrain neurogenesis and striatal neuron replacement after focal stroke. *Ann. Neurol.* **52**, 802–813 (2002).
18. Zhang, R. L., Zhang, Z. G., Zhang, L. & Chopp, M. Proliferation and differentiation of progenitor cells in the cortex and the subventricular zone in the adult rat after focal cerebral ischemia. *Neuroscience* **105**, 33–41 (2001).
19. Thored, P. *et al.* Persistent Production of Neurons from Adult Brain Stem Cells During Recovery after Stroke. *Stem Cells* **24**, 739–747 (2005).
20. Thored, P. *et al.* Long-term neuroblast migration along blood vessels in an area with transient angiogenesis and increased vascularization after stroke. *Stroke* **38**, 3032–3039 (2007).
21. Ohab, J. J., Fleming, S., Blesch, A. & Carmichael, S. T. A Neurovascular Niche for

Neurogenesis after Stroke. *J. Neurosci.* **26**, 13007–13016 (2006).

22. Yamashita, T. *et al.* Subventricular Zone-Derived Neuroblasts Migrate and Differentiate into Mature Neurons in the Post-Stroke Adult Striatum. *J. Neurosci.* **26**, 6627–6636 (2006).

23. Ohira, K. *et al.* Ischemia-induced neurogenesis of neocortical layer 1 progenitor cells. *Nat. Neurosci.* **13**, 173–179 (2010).

24. Hara, T. *et al.* Molecular cloning and functional characterization of a novel member of the C-C chemokine family. *J. Immunol.* **155**, 5352–8 (1995).

25. Barkho, B. Z. & Zhao, X. Adult neural stem cells: response to stroke injury and potential for therapeutic applications. *Curr. Stem Cell Res. Ther.* **6**, 327–38 (2011).

26. Kitamura, T. *et al.* SMAD4-deficient intestinal tumors recruit CCR1+ myeloid cells that promote invasion. *Nat. Genet.* **39**, 467–475 (2007).

27. Hwang, J. *et al.* Angiogenic activity of human CC chemokine CCL15 in vitro and in vivo. *FEBS Lett.* **570**, 47–51 (2004).

28. Li, Y. S., Gurrieri, M. & Deuel, T. F. Pleiotrophin gene expression is highly restricted and is regulated by platelet-derived growth factor. *Biochem. Biophys. Res. Commun.* (1992). doi:10.1016/0006-291X(92)91211-8

29. Courty, J., Claude Dauchel, M., Caruelle, D., Perderiset, M. & Barritault, D. Mitogenic properties of a new endothelial cell growth factor related to pleiotrophin. *Biochem. Biophys. Res. Commun.* **180**, 145–151 (1991).

30. Besse, S. *et al.* Pleiotrophin promotes capillary-like sprouting from senescent aortic rings. *Cytokine* **62**, 44–47 (2013).

31. Relf, M. *et al.* Expression of the angiogenic factors vascular endothelial cell growth

factor, acidic and basic fibroblast growth factor, tumor growth factor β-1, platelet-derived endothelial cell growth factor, placenta growth factor, and pleiotrophin in human primary br. *Cancer Res.* **57**, 963–969 (1997).

32. GonzÃ¡lez-Castillo, C., OrtuÃ±o-SahagÃºn, D., GuzmÃ¡n-Brambila, C., PallÃ s, M. & Rojas-MayorquÃ-n, A. E. Pleiotrophin as a central nervous system neuromodulator, evidences from the hippocampus. *Front. Cell. Neurosci.* **8**, 1–7 (2015).
33. Yeh, H.-J., He, Y. Y., Xu, J., Hsu, C. Y. & Deuel, T. F. Upregulation of Pleiotrophin Gene Expression in Developing Microvasculature, Macrophages, and Astrocytes after Acute Ischemic Brain Injury. *J. Neurosci.* **18**, 3699–3707 (2018).
34. Daneman, R. *et al.* Wnt/ -catenin signaling is required for CNS, but not non-CNS, angiogenesis. *Proc. Natl. Acad. Sci.* **106**, 641–646 (2009).
35. Qu, Q. *et al.* Wnt7a Regulates Multiple Steps of Neurogenesis. *Mol. Cell. Biol.* **33**, 2551–2559 (2013).
36. McLean, I. W. & Nakane, P. K. Fixative Microscopy. *J. Histochem. Cytochem.* **22**, 1077–83 (1974).
37. Fluri, F., Schuhmann, M. K. & Kleinschnitz, C. Animal models of ischemic stroke and their application in clinical research. *Drug Des. Devel. Ther.* **9**, 3445–3454 (2015).
38. Duan, X., Kang, E., Liu, C. Y., Ming, G. li & Song, H. Development of neural stem cell in the adult brain. *Curr. Opin. Neurobiol.* **18**, 108–115 (2008).
39. Engelhardt, B. Development of the blood-brain barrier. *Cell Tissue Res.* **314**, 119–129 (2003).
40. Blood, T., Barrier, B., Daneman, R. & Prat, A. The Blood –Brain Barrier. 1–23 (2015).
41. Cornford, E. M., Hyman, S. & Swartz, B. E. The human brain GLUT1 glucose

transporter: Ultrastructural localization to the blood-brain barrier endothelia. *J. Cereb. Blood Flow Metab.* **14**, 106–112 (1994).

42. Sunnemark, D. *et al.* Differential Expression of the Chemokine Receptors CX3CR1 and CCR1 by Microglia and Macrophages in Myelin-Oligodendrocyte-Glycoprotein-Induced Experimental Autoimmune Encephalomyelitis. *Brain Pathol.* **13**, 617–629 (2006).

43. Ohab, J. J. & Carmichael, S. T. Poststroke neurogenesis: Emerging principles of migration and localization of immature neurons. *Neuroscientist* **14**, 369–380 (2008).

44. Kreuzberg, M. *et al.* Increased subventricular zone-derived cortical neurogenesis after ischemic lesion. *Exp. Neurol.* **226**, 90–99 (2010).

45. Daneman, R. The blood-brain barrier in health and disease. *Ann. Neurol.* (2012). doi:10.1002/ana.23648

46. Jiang, X. *et al.* Blood-brain barrier dysfunction and recovery after ischemic stroke. *Prog. Neurobiol.* **163**–**164**, 144–171 (2018).

47. Prakash, R. & Carmichael, S. T. Blood-brain barrier breakdown and neovascularization processes after stroke and traumatic brain injury. *Curr. Opin. Neurol.* **28**, 556–564 (2015).

48. Qu, Q. *et al.* Orphan nuclear receptor TLX activates Wnt/B-catenin signalling to stimulate neural stem cell proliferation and self-renewal. *Nat. Cell Biol.* **12**, 31–40 (2010).

49. Prajerova, I., Honsa, P., Chvatal, A. & Anderova, M. Distinct effects of Sonic hedgehog and Wnt-7a on differentiation of neonatal neural stem/progenitor cells in vitro. *Neuroscience* **171**, 693–711 (2010).

50. Adachi, K. *et al.* β-Catenin Signaling Promotes Proliferation of Progenitor Cells in the Adult Mouse Subventricular Zone. *Stem Cells* **25**, 2827–2836 (2007).

51. Wodarz, A. & Nusse, R. Mechanisms of Wnt signaling in development. *Annu. Rev. Cell*

*Dev. Biol.* **14**, 59–88 (1998).

52. McCormick, F. & Tetsu, O. Beta-Catenin regulates expression of cyclin D1 in colon carcinoma cells. *Nature* **398**, 422–426 (1999).

53. Ahmad-Annuar, A. *et al.* Signaling across the synapse: A role for Wnt and Dishevelled in presynaptic assembly and neurotransmitter release. *J. Cell Biol.* **174**, 127–139 (2006).

54. Cerpa, W. *et al.* Wnt-7a modulates the synaptic vesicle cycle and synaptic transmission in hippocampal neurons. *J. Biol. Chem.* **283**, 5918–5927 (2008).

55. Ciani, L. *et al.* Wnt7a signaling promotes dendritic spine growth and synaptic strength through Ca2+/Calmodulin-dependent protein kinase II. *Proc. Natl. Acad. Sci.* **108**, 10732–10737 (2011).

56. Hall, A. C., Lucas, F. R. & Salinas, P. C. Axonal Remodeling and Synaptic Differentiation in the Cerebellum Is Regulated by WNT-7a Signaling becomes multilobulated as it interdigitates with GC den- drites (Hamori and Somogyi, 1983). The increase in mossy fiber surface area permits the formation of. *Cell* **100**, 525–535 (2000).

57. Lucas, F. R. & Salinas, P. C. WNT-7a induces axonal remodeling and increases synapsin I levels in cerebellar neurons. *Dev. Biol.* **192**, 31–44 (1997).

58. Gogolla, N., Galimberti, I., Deguchi, Y. & Caroni, P. Wnt Signaling Mediates Experience-Related Regulation of Synapse Numbers and Mossy Fiber Connectivities in the Adult Hippocampus. *Neuron* **62**, 510–525 (2009).

59. Li, Y. S. *et al.* Cloning and expression of a developmentally regulated protein that induces mitogenic and neurite outgrowth activity. *Science (80-. ).* **250**, 1690 LP – 1694 (1990).

60. Mentlein, R. & Held-Feindt, J. Pleiotrophin, an angiogenic and mitogenic growth factor, is expressed in human gliomas. *J. Neurochem.* **83**, 747–753 (2002).

61. Lin, T. N., Te, J., Lee, M., Sun, G. Y. & Hsu, C. Y. Induction of basic fibroblast growth factor (bFGF) expression following focal cerebral ischemia. *Mol. Brain Res.* **49**, 255–265 (1997).

62. Meng, K. *et al.* Pleiotrophin signals increased tyrosine phosphorylation of beta -catenin through inactivation of the intrinsic catalytic activity of the receptor-type protein tyrosine phosphatase beta /zeta. *Proc. Natl. Acad. Sci.* **97**, 2603–2608 (2000).

63. Yang, L. *et al.* Expansion of myeloid immune suppressor Gr+CD11b+ cells in tumor-bearing host directly promotes tumor angiogenesis. *Cancer Cell* **6**, 409–421 (2004).

64. Perry, V. H. & Teeling, J. Microglia and macrophages of the central nervous system: The contribution of microglia priming and systemic inflammation to chronic neurodegeneration. *Semin. Immunopathol.* **35**, 601–612 (2013).

65. Kortlever, R. M. *et al.* Myc Cooperates with Ras by Programming Inflammation and Immune Suppression. *Cell* **171**, 1301-1315.e14 (2017).

66. Wang, Q., Tang, X. N. & Yenari, M. A. The inflammatory response in stroke. *J. Neuroimmunol.* **184**, 53–68 (2007).

67. Chen, Y. *et al.* Overexpression of monocyte chemoattractant protein 1 in the brain exacerbates ischemic brain injury and is associated with recruitment of inflammatory cells. *J. Cereb. Blood Flow Metab.* **23**, 748–755 (2003).

68. Cartier, L., Hartley, O., Dubois-Dauphin, M. & Krause, K. H. Chemokine receptors in the central nervous system: Role in brain inflammation and neurodegenerative diseases. *Brain Res. Rev.* **48**, 16–42 (2005).

69. Kitamura, T. *et al.* Inactivation of chemokine (C-C motif) receptor 1 (CCR1) suppresses colon cancer liver metastasis by blocking accumulation of immature myeloid cells in a

mouse model. *Proc. Natl. Acad. Sci.* **107**, 13063–13068 (2010).

70. Moelants, E. A. V, Mortier, A., Van Damme, J. & Proost, P. In vivo regulation of chemokine activity by post-translational modification. *Immunol. Cell Biol.* **91**, 402–407 (2013).

71. Burkle, A. Posttranslational Modification Predator ± Prey and Parasite ± Host Interactions. in *Encyclopedia of Genetics* (2001). doi:10.1006/rwgn.2001.1022